Available online at www.sciencedirect.com
ScienceDirect
Sedimentary Geology 202 (2007) 96–123
Sedimentary Geology
www.elsevier.com/locate/sedgeo

Volcanic and climatic controls on fluvial style in a high-energy system: The Lower Cretaceous Matasiete Formation, Golfo San Jorge basin, Argentina

José Matildo Paredes [a,*], Nicolás Foix [a], Ferrán Colombo Piñol [b], Adriana Nillni [a], José O. Allard [a], Rosa A. Marquillas [c]

[a] *Dpto. de Geología, F.C.N., Universidad Nacional de la Patagonia "San Juan Bosco", Ruta Provincial N° 1, Km. 4, (9005) Comodoro Rivadavia, Chubut, Argentina*
[b] *Dpto. de Estratigrafía, Paleontología y Geociencias Marinas, Fac. de Geología, Universidad de Barcelona, 08071, Barcelona, Spain*
[c] *CONICET, Dpto. de Geología, F.C.N., Universidad Nacional de Salta, Buenos Aires 177 (4400) Salta, Argentina*

Abstract

The Cretaceous Chubut Group in the Golfo San Jorge Basin (Patagonia, Argentina) comprises up to 6000 m of continental sediments. At the base of the succession, an extensive saline–alkaline lacustrine unit (Pozo D-129 Fm) grades laterally towards the basin margin into the fluvial Matasiete Fm (Hauterivian?–Aptian). The Matasiete Fm comprises up to 650 m of siliciclastic and pyroclastic deposits in its type area, where three Members have been distinguished. The following facies associations were identified: 1) single fluvial channels; 2) multistorey fluvial channels; 3) proximal floodplain; 4) distal floodplain; 5) pyroclastic (ash-fall and ground-surge) deposits. Additional observations in the time-equivalent Pozo D-129 Fm provide evidence for 6) shallow lacustrine, and 7) deep-lacustrine facies associations. The floodplain association contains paleosols with abundant carbonate concretions and fine pyroclastic tuffs. Paleosols are mostly vertisols, characterized by deep desiccation cracks, slickensides and carbonate nodules. These observations, coupled with the occurrence of shallow-water oolitic grainstones in the lacustrine Pozo D-129 Fm indicate a semiarid environment. Tree trunks up to 1 m in diameter and 15 m long, preferentially located near channel margins, provide evidence for vegetated riverbanks. The exposures of the Matasiete formation in the San Bernardo Fold Belt show individual channel belts containing straight, meandering and braided channels. Evidence of changes in fluvial style attributable to base-level control has not been observed. The most dramatic changes in fluvial architecture, which were comparatively short-lived, were provoked by intermittent pyroclastic deposition on the floodplain. The reduced infiltration capacity of the floodplain and the concomitant increase in sediment load increased runoff, as well as volume and flashiness of the discharge, which favoured the development of shallow, multichannel rivers. The fluvial system abruptly changed from single, ribbon channels to a braided system, which notably increased the width/thickness ratio of sandbodies.

Keywords: High-energy fluvial systems; Fluvial architecture; Pyroclastic input; Climatic and volcanic controls; Cretaceous; Patagonia; Argentina

1. Introduction

Understanding of the evolution of river systems requires reconstruction of changes in depositional environments in space and time. Such reconstructions

* Corresponding author. Tel.: +54 297 154 125 039; fax: +54 297 455 0339.
E-mail address: paredesj@unpata.edu.ar (J.M. Paredes).

0037-0738/$ - see front matter © 2007 Elsevier B.V. All rights reserved.
doi:10.1016/j.sedgeo.2007.05.007

must be based on detailed measurements of parameters related to the hydrological behaviour of channel belts and the associated floodplain, as well as the correct recognition of changes in external controls on sedimentation (e.g. base level, tectonics, climate, and volcanism). In recent years, a number of seminal papers have addressed changes in fluvial architecture produced under conditions of tectonic forcing (e.g. Bridge and Leeder, 1979; Alexander and Leeder, 1987; Schumm, 1993; Holbrook and Schumm, 1999; Arche and Lopez-Gomez, 1999; Gawthorpe and Leeder, 2000), base-level changes (Legarreta et al., 1993; Wright and Marriot, 1993; Shanley and McCabe, 1994; Emery and Myers, 1996; Leeder and Steward, 1996; Legarreta and Uliana, 1998; Shanley and McCabe, 1998; Kraus, 1999), and subtle changes in climate of source areas and alluvial basins (Shanley and McCabe, 1998; Blum and Tornqvist, 2000; Cecil, 2003). The dramatic impact of pyroclastic input into the drainage system and the floodplain, particularly relevant for basins located near areas of volcanic activity, has also been evaluated in the last decades (Cas and Wright, 1987; Smith, 1987; Fisher and Smith, 1991).

This work seeks to contribute to the insights obtained in the above studies, by unravelling the controls on sedimentology, stratigraphy and depositional architecture of the fluvial systems of the Matasiete Formation, based on detailed field observations in the San Bernardo Fold Belt. Particular attention has been given to the role of pyroclastic input and its effects on fluvial architecture. A regional framework for synthesizing the controls on deposition has been constructed by means of additional observations on the lacustrine Pozo D-129 Fm, which comprises deposits of a lake that acted as a regional base level for the fluvial systems.

1.1. Stratigraphic and tectonic setting

The Chubut Group of the Golfo San Jorge basin provides a record of fluvial and lacustrine deposition in an intracratonic setting. The deposits reach about 6000 m in thickness in the subsurface of the basin, and comprise around 2000 m of epiclastic and pyroclastic deposits along the San Bernardo Fold Belt (Fig. 1), a North–South trending belt in which extensional Mesozoic faults were inverted mostly during the Tertiary (Homovc et al., 1995). In recent decades, detailed investigations of the Chubut Group have been carried out, mostly due to their importance for the oil industry. The Pozo D-129 Fm is considered to be the main source rock of the basin, and the volcaniclastic sandstones of the Castillo and Bajo Barreal Fms are the main oil reservoir rocks.

The "Neocomiano" or Las Heras Group (Fig. 2), a marine to transitional megasequence deposited under synrift conditions (Figari et al., 1999) underlies the Chubut Group. The Las Heras Group is not exposed in the San Bernardo Fold Belt. The Tertiary sediments that cover the Chubut Group consist of fluvial and aeolian deposits preserved in local depressions, and scarce marine sediments preserved in the southern part of the Fold Belt. The lithostratigraphic arrangement of the Chubut Group indicates the development of an extensive saline–alkaline lacustrine unit at the base (Pozo D-129 Fm), which is laterally equivalent to the fluvial Matasiete Fm (Hauterivian? to Aptian). The Castillo Fm, a volcaniclastic unit deposited in fluvial and very shallow lacustrine environments during the Albian, conformably covers both units. The Chubut Group also contains younger fluvial deposits of the Bajo Barreal Fm (Cenomanian to Campanian) and the Laguna Palacios Fm (Santonian to Maastrichtian), the latter characterized by stacked paleosols and minor channels.

Regional studies of the Golfo San Jorge basin based on subsurface and outcrop data (Barcat et al., 1989; Fitzgerald et al., 1990; Peroni et al., 1995; Figari et al., 1999; Uliana and Legarreta, 1999; Hechem and Strelkov, 2002) have depicted the general evolution of the basin and its petroleum systems. Fitzgerald et al. (1990) regarded the Pozo D-129 Fm as part of an early sag stage in the evolution of the basin, whereas other authors (Figari et al., 1999) proposed an extensional or transtensional setting during deposition of the Pozo D-129 Formation. Thermal subsidence has been the main mechanism during deposition of the other units of the Chubut Group (Figari et al., 1999; Rodriguez and Littke, 2001). Feruglio (1949), Lesta and Ferello (1972), Sciutto (1981), Clavijo (1986) and Hechem et al. (1990) formulated the main characteristics and stratigraphic relationship of the Chubut Group. Hechem et al. (1990) recognized six depositional sequences in the Chubut Group. The lower three depositional sequences include the Pozo D-129, Matasiete and Castillo Fms, characterized by the development of a fluvial and lacustrine environment, in which transgressive to regressive cycles are attributed to changes in tectonically and/or climatically forced changes in lake size. The upper three depositional sequences are represented by the Bajo Barreal and Laguna Palacios Fms. Both consist of volcaniclastic beds and braided ephemeral fluvial deposits (Hechem et al., 1990).

Detailed stratigraphic studies in selected outcrops of the Castillo and Bajo Barreal Fms have been carried out during the past two decades (Meconi, 1990; Rodriguez, 1992; Legarreta et al., 1993; Hechem, 1994, 1998; Bridge

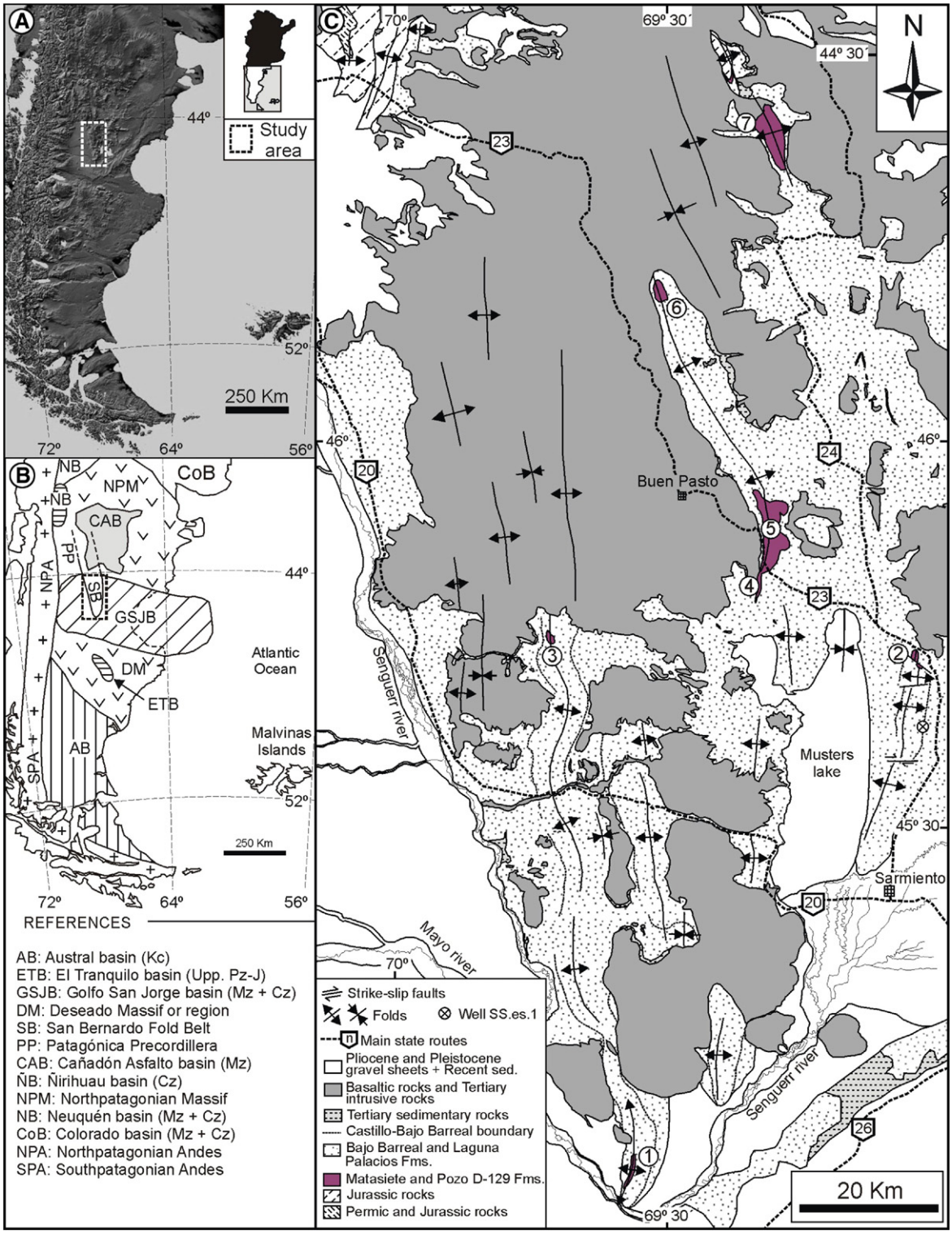

Fig. 1. Location of the Golfo San Jorge basin in central Patagonia, and the study area. A) Radar image of Patagonia, the boxed area marks the location of the San Bernardo Fold Belt. B) Sedimentary basins and uplifted areas in Patagonia. C) Geological map of the San Bernardo Fold Belt, with indication of the exposures of the Matasiete and Pozo D-129 Fms. Both units are exposed in the cores of anticlines. 1) Codo del Senguerr Anticline, 2) Chenque (Silva) Hill, 3) Cachetamán Hill, 4) Baya Peninsula, 5) Matasiete Canyon, 6) Sierra Nevada Anticline, 7) Tronador Canyon. Basaltic and intrusive rocks (Eocene-recent) cover most of the San Bernardo Fold Belt area. Paleozoic and Jurassic rocks in the northern part of the fold belt represent deposits of a previous basin.

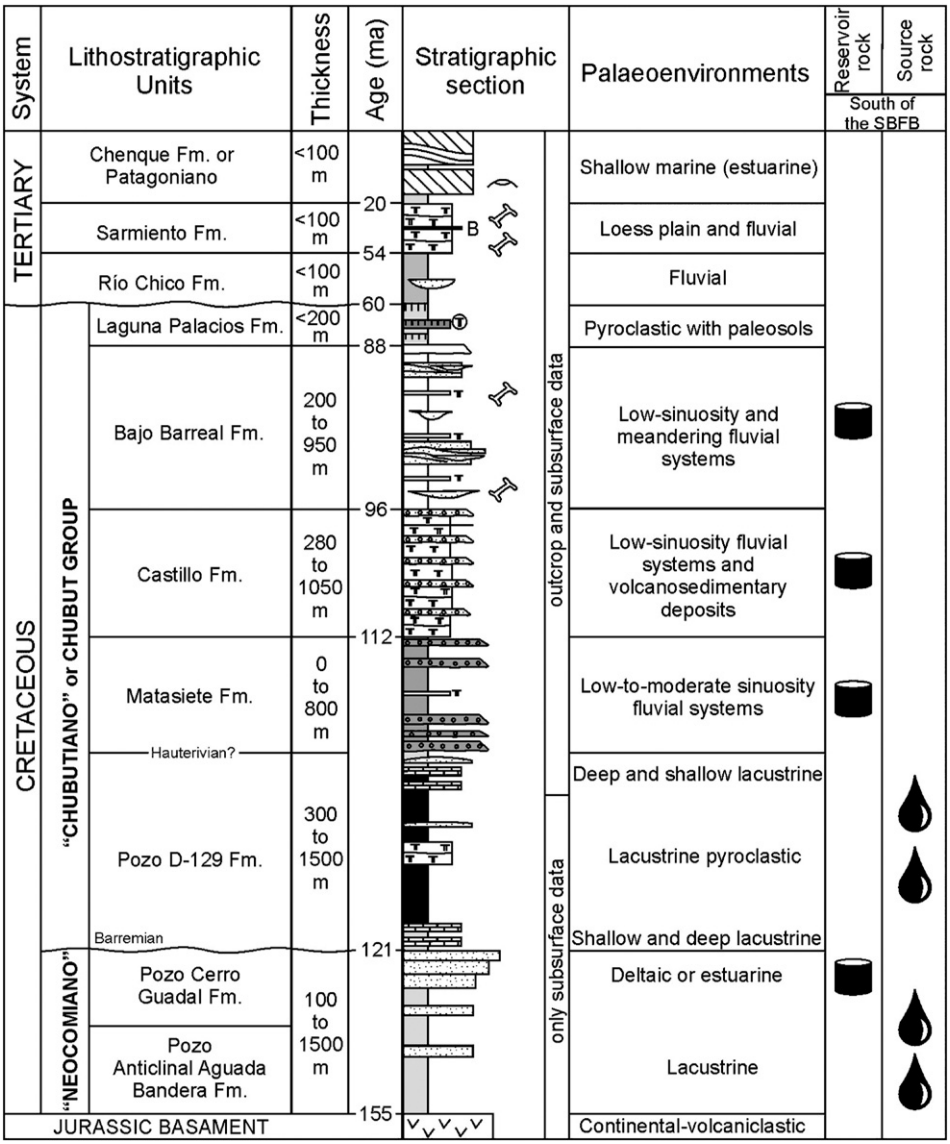

Fig. 2. Synthetic lithostratigraphy and palaeoenvironments of the San Bernardo Fold Belt. Ages according to Fitzgerald et al. (1990), Bridge et al. (2000) and Rodriguez and Littke (2001).

et al., 2000). The paper of Bridge et al. (2000) is, until now, the most detailed work on fluvial architecture developed in the Chubut Group. Their work was focused on outcrops of the Bajo Barreal Fm and part of the Castillo Fm, in exposures mostly southward of the study area of the present paper. They found evidence of perennial fluvial systems with straight channels (sinuosity less than 1.23) and rare braided channels, and mean thickness in the order of 2 to 5 m, but variable between the studied areas (Bridge et al., 2000). Previously published data from the Matasiete Fm in the Matasiete Canyon (Paredes et al., 2003) were used in the present study of this unit over the entirety of the San Bernardo Fold Belt.

1.2. The Pozo D-129 and Matasiete depositional system

The Matasiete and Pozo D-129 units are exposed in the San Bernardo Fold Belt as isolated outcrops in the cores of asymmetrical anticlines (Fig. 1). The lacustrine Pozo D-129 Fm is exposed in the Codo del Senguerr anticline, Silva Hill and Baya Peninsula. The base of the unit is not exposed in the basin, and the stratigraphic interval exposed in individual outcrops does not exceed 100 m. However, in the subsurface of surrounding areas (e.g. Well Ch-SS.es.1) its thickness exceeds 900 m. A thickness of at least 1500 m commonly occurs in the areas to the South and East of the San Bernardo Fold

Belt (Figari et al., 1999). Because of the scarcity of exposures of lacustrine rocks, their subdivision is based on subsurface data. Regional facies distribution in the lacustrine Pozo D-129 Fm suggests a provenance of clastics from the North Patagonian and Deseado regions (Fig. 3, after Figari et al., 1999), in an East–West elongate basin with main depocenters parallel to major normal faults. An increase in pyroclastic content towards the western sector was attributed to early volcanic activity in the Andean Ranges (Folguera and Iannizzotto, 2004).

Clavijo (1986) informally identified four main units (sections) in the Pozo D-129 Fm of the western part of the basin. The lower section contains tuffs and tuffaceous siltstones, grey-to-green laminated shales, and a subordinate amount of sandstones deposited in deep-lacustrine environments. This evolves upwards into pale grey tuffs containing thin tuffaceous sandstones and oolitic grainstones, which represent deposition in littoral shoals. A section dominated by stacked green tuffs with minor coarse-to-medium-grained tuffaceous sandstones, considered to be shallow lacustrine deposits with high pyroclastic content, occurs higher up in the unit. Finally, an upper section composed of white tuffs containing sandstones, minor oolitic grainstones and green tuffaceous sandstones was recognized, inferred to have been deposited in a marginal to fluvio-deltaic environment (Clavijo, 1986).

Anoxic conditions have been inferred for different sections of the Pozo D-129 Fm, based on the presence of

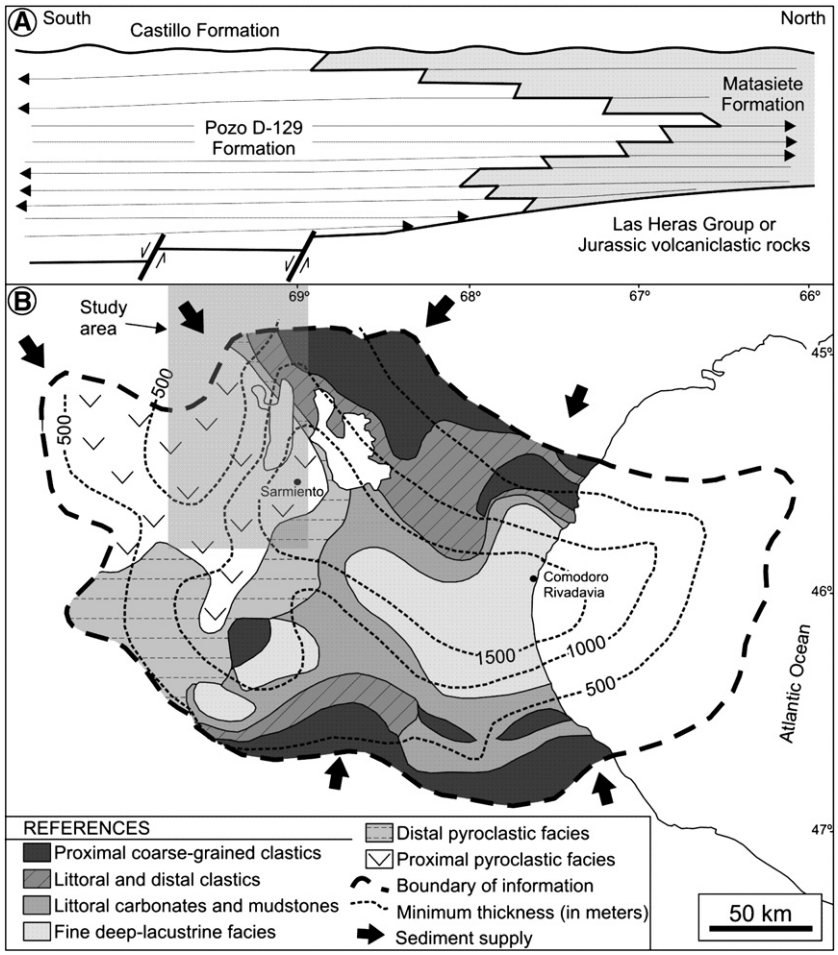

Fig. 3. Regional patterns of the Matasiete and Pozo D-129 Fms. A) Lateral relationship between Pozo D-129 and Matasiete Fms, showing thickness variation from North to South and the main progradational–retrogradational cycles (modified from Hechem and Strelkov, 2002). B) Regional distribution of the Pozo D-129 Fm and lithological character of the unit, mainly based on subsurface information. Coarse clastics were mostly provided from the North Patagonian and Deseado regions. Pyroclastic material from the former Andes Ranges is most abundant in the western part of the area. Local source areas are marked by the presence of coarse clastics (after Figari et al., 1999).

laminated shales containing pyrite, dark colors and absence of burrows (Van Nieuwenhuise and Ormiston, 1989). The dominance of *Classopolis* pollen and the abundance of oolitic grainstones, as well as the presence of *Botryococcus*-like algal forms, led these authors to suggest that deposition occurred in a stratified saline–alkaline lacustrine system in a semiarid climate. The Barremian to Aptian age assigned to the unit was based on the presence of the *Flabellochara harrisi* association, obtained from outcrops of the Chenque (Silva) Hill (Hechem et al., 1987), but some studies support an Hauterivian age for the beginning of lacustrine deposition (Archangelski et al., 1984; Fitzgerald et al., 1990).

The Matasiete Fm (Lesta and Ferello, 1972) was originally named "Reddish Sandstones and Tuffs" by Feruglio (1949). Lesta and Ferello (1972) identified three Members (Lower, Middle and Upper) based on the ratio of sandstone bodies to floodplain suites. Sciutto (1981) provided details of the distribution of these units in outcrops of the San Bernardo Fold Belt and commented on their main characteristics. This author was the first to recognize the lateral relation between the Matasiete Fm and the lacustrine Pozo D-129 Fm, and interpreted the former as a meandering high-energy fluvial system. Galeazzi (1989) described the sedimentology of the Matasiete Fm in the southern part of Matasiete Canyon, and proposed a subdivision of this formation into two depositional sequences (the Lower and Middle Members are included in Sequence 1 and the Upper Member is equivalent to Sequence 2). He attributed changes in channel geometry within the Matasiete Fm to base-level variations. The fluvial systems were considered to be braided in the lower sequence and fully lacustrine to meandering in the upper sequence with paleocurrents to the southeast (~120°) (Galeazzi, 1989). Paredes et al. (2003, 2004) recognized the large variability in fluvial deposits within individual Members and between superimposed channel belts, and highlighted the variation in paleocurrent directions, the dominance of channel migration by avulsion, and the presence of large tree trunks in some of the channel fills (some 1 m in thick and 15 m long). Paredes et al. (2003, 2004), who analyzed the lithostratigraphy of the Matasiete Formation in and around its type area, showed the Lower Member to be composed of a 205 m thick section deposited by a low-sinuosity fluvial system with three main channel belts, separated by floodplain fines. The Middle Member is 215 m thick, and characterized by the dominance of floodplain fines over channel fills. The fluvial system provides evidence of meandering and braided behaviour, but many sandbodies have no diagnostic features. The Middle Member of the Matasiete Fm grades laterally in a southward direction to lacustrine facies of the Pozo D-129 Fm (Hechem et al., 1990; Hechem and Strelkov, 2002; Paredes et al., 2003). The Upper Member, which regionally covers the lacustrine Pozo D-129 Fm, consists of a 230 m thick section of red-coloured fluvial deposits comprising straight, meandering and braided channel fills.

2. Materials and methods

This study comprises the description and interpretation of detailed stratigraphic sections of the Matasiete Fm in seven areas of the San Bernardo Fold Belt (Figs. 4 and 5), and analysis of additional observations from the lacustrine Pozo D-129 Fm. Three Members were proposed in the Matasiete Canyon based on grain-size analysis and facies assemblages (Lesta and Ferello, 1972), and all references in the present study to Lower, Middle and Upper Members of the Matasiete Fm are indexed to this scheme. All three Members are exposed in the Matasiete Canyon (Fig. 5). In the other areas there are only exposures of the Upper Member of the Matasiete Fm or the lacustrine Pozo D-129 Fm (Fig. 4).

The term sandbody is used in a general sense and includes single and multistorey channel fills. The architectural elements of Miall (1996) and their bounding surfaces were deduced from interpretation of outcrop profiles and photomosaics of laterally continuous outcrops. Paleocurrent directions were measured from unidirectional sedimentary structures such as cross-stratification, asymmetrical ripples or oriented tree trunks, and were structurally corrected (Ramsay, 1961). The apparent dimensions of channel fills were measured using GPS point data along the edges of sandbodies, and corrected with the mean of the paleocurrent data for each channel fill. The lithofacies analysis largely follows the classifications and facies definitions of Miall (1996), Bridge (1993) and Talbot and Allen (1996), with modifications for volcaniclastic environments suggested by Mathisen and Vondra (1983), Smith (1987) and Cas and Wright (1987). Thin sections were obtained from most of the lithofacies and from the unit exposed in the Matasiete Canyon. Paleosol analysis included a description of color, grain size, nodule type, as well as matrix and mottles. Determination of major oxide weight percent was carried out by X-ray fluorescence of whole-rock samples. Clay minerals were identified by X-ray diffraction.

3. Sedimentology

Galeazzi (1989) and Paredes et al. (2003) proposed lithofacies schemes for the Matasiete Fm based on

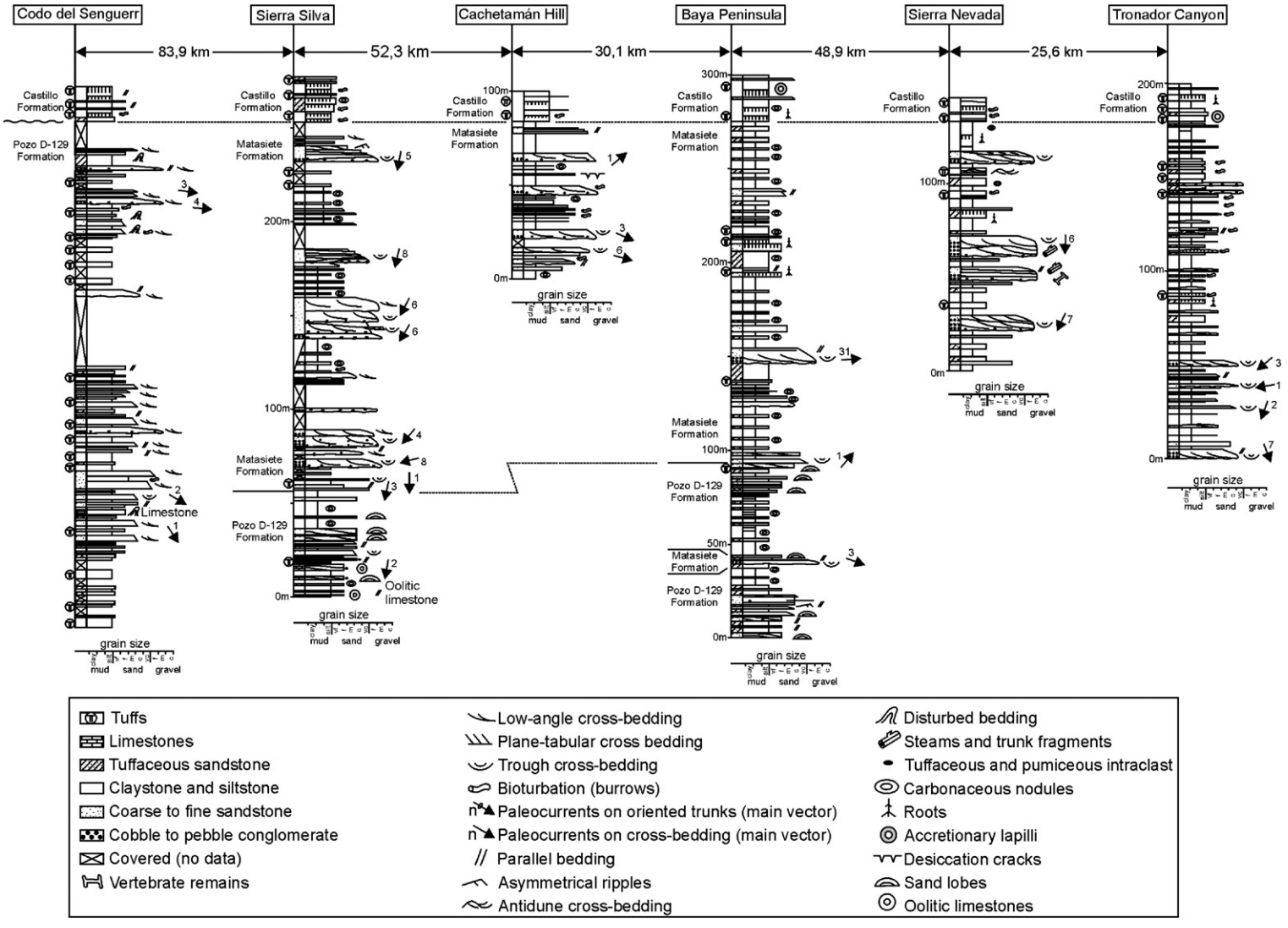

Fig. 4. Stratigraphic sections of the Upper Member of the Matasiete Fm and lacustrine Pozo D-129 Fm. Location of the sections in Fig. 1C. The most complete section of the unit is exposed in the Matasiete Canyon (Fig. 5).

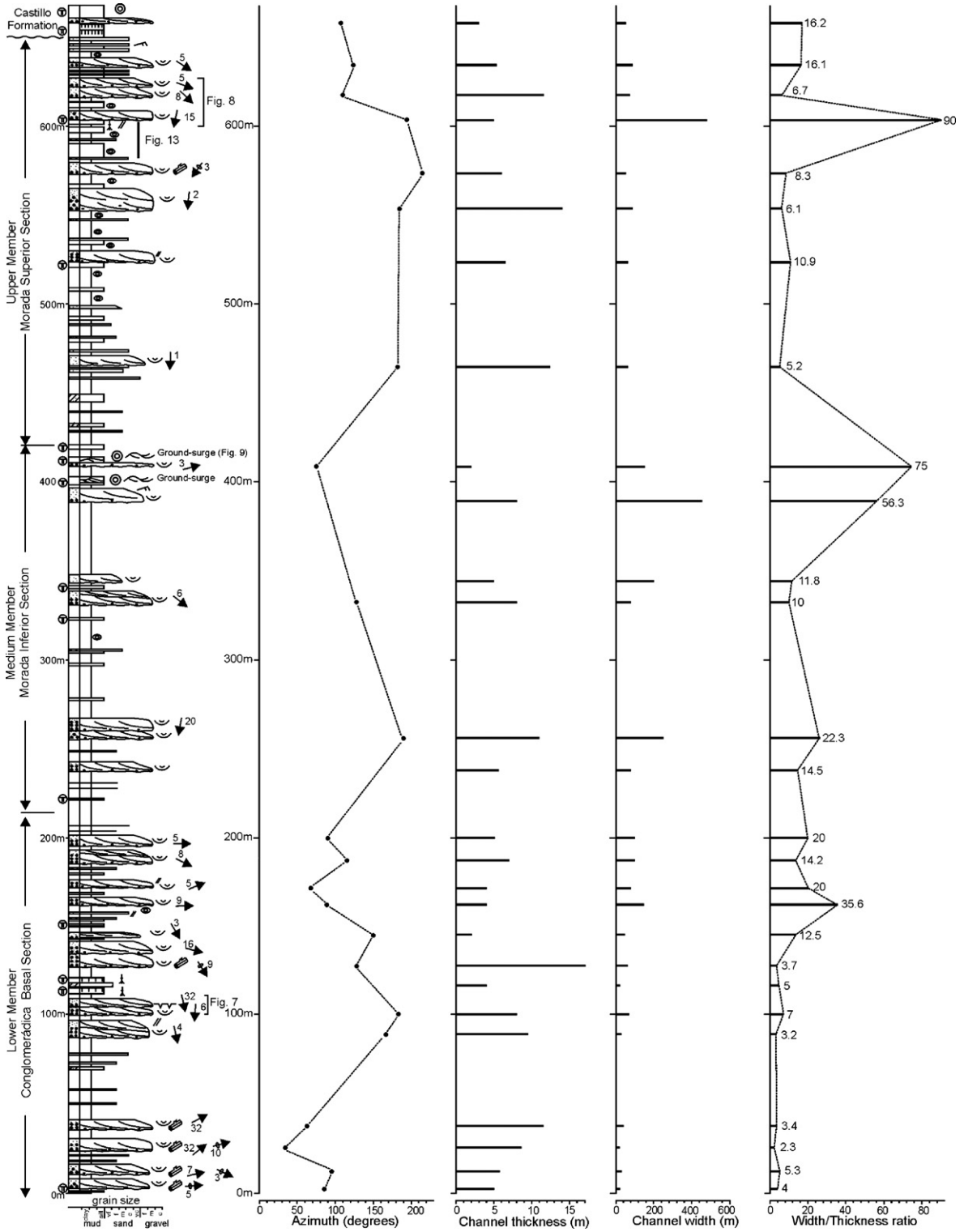

Fig. 5. Synthetic stratigraphic section of the Matasiete Fm at Matasiete Canyon. The Lower, Middle and Upper members are defined according to the ratio of floodplain fines over channelized facies. The stratigraphic distribution of the sandbodies and their *W*/*T* ratio is indicated (modified from Paredes et al., 2003).

exposures in the Matasiete Canyon. As new observations allowed us to identify new lithofacies and depositional processes, short descriptions of the lithofacies are presented in Table 1 and Fig. 6. Five genetically significant lithofacies associations were identified in the Matasiete Fm with the aid of textures, sedimentary structures, geometry, paleocurrent indicators and lateral and vertical arrangement of lithofacies: 1) single fluvial channels; 2) multistorey fluvial channels; 3) proximal floodplain; 4) distal floodplain; 5) pyroclastic deposits. Two additional lithofacies associations were distinguished in the time-equivalent lacustrine Pozo D-129 Fm: 6) shallow lacustrine association and 7) deep-lacustrine association.

3.1. Facies association of the Matasiete Fm

3.1.1. Facies association 1: single fluvial channels

3.1.1.1. Description. Facies association (FA) 1 consists of lenticular beds of sandstone less than 3 m thick and a few tens of meters in width, encased in red mudstone. The sandbodies are characterized by the absence of lateral accretion surfaces. The channel fills have a low relief basal erosion surface, do not fine upward significantly, and are volumetrically dominated by matrix-supported fine conglomerates and sandstones (Facies LF1), and clast-supported conglomerates, either horizontally bedded (Facies FL2) or containing trough cross-bedding (Facies LF3). Paleocurrent directions obtained from cross-strata, and tree trunks generally show low dispersion (<50°) around the mean. Occasionally, consecutive channels in a single section show orthogonal palaeotransport directions.

3.1.1.2. Interpretation. Deposition in single-thread fluvial channels is indicated by a significant basal erosion surface, lenticular geometry, coarse infilling and unidirectional paleocurrents. Single episodes of deposition are suggested by the lack of internal erosion surfaces and by uniformity in thickness of cross-sets that fill the channels (Lunt et al., 2004). Paleoflow variation between channels is attributed to tectonic tilting or nodal avulsions. The absence of lateral accretion surfaces implies that the channels were laterally stable.

3.1.2. Facies association 2: multistorey fluvial channels

3.1.2.1. Description. Facies association (FA) 2 consists of erosionally-based, lenticular and tabular sandbodies 3 to 20 m thick, with multiple internal erosion surfaces. Most sandbodies lack lateral accretion surfaces, have ribbon geometries and internally comprise 3 to 4, slightly laterally shifted, vertically stacked stories (e.g. Fig. 7). They mostly comprise clast-supported conglomerate, either horizontally bedded (Facies LF2) or containing trough cross-bedding (Facies LF3), with matrix-supported conglomerate and sandstone (Facies LF1), features shared with FA1. The upper parts of the sandbodies are dominated by coarse-grained sandstones with low-angle cross bedding, trough and planar cross-bedding (Facies LF3 and LF4), and occasional medium-grained sandstones with asymmetrical ripples (Facies LF6). In some cases, sandstones with desiccation cracks (Facies LF5) were observed on the upper surfaces of fining-upward sandbodies (e.g. Fig. 7). The general trend of the channel fills is fining-upward, but many strata show no vertical grain-size trend. Where fining-upward trend is preserved, there is also a decrease in bedform height and bed thickness upward. Thicknesses of cross-beds range from 0.3 to 1.8 m. They show unimodal paleocurrent directions with generally low dispersion. Internal erosional surfaces are gently concave upwards, show scours in the scale of tens of centimeters and are filled by a thick, poorly organized lag and low-angle, horizontally bedded conglomerates (Facies LF2). Occasional tree-trunk fragments, are 30 to 50 cm in diameter (maximum observed diameter was 1 m) and 4 to 15 m long. The larger trunks are oriented parallel to the channel margins and slightly inclined in opposed direction to the flow. Few multistorey sandbodies have several large-scale inclined surfaces containing trough cross-bedding and asymmetrical ripples (Facies LF7) on top. Single stories in the later sandbodies are separated by pale grey, laminated mudstones (Fig. 8). The tabular sandbody emplaced on the regional tuff bed of Fig. 8 preserves a convex-upward, large-scale inclined surface in a direction normal to the measured paleocurrent.

3.1.2.2. Interpretation. The coarse-grain size, basal and internal erosional surfaces, unimodal paleocurrents, trough and planar cross-stratification in sandstone up to massive conglomerate beds, compound cross-strata and the absence of marine fossils suggest deposition in multistorey fluvial channels (Bridge, 1993; Miall, 1996). Some elongate sheets of conglomerate containing horizontal bedding (Facies LF2) represent longitudinal bedforms. The trough-cross stratified conglomerates and sandstones (Facies LF3) were deposited in 3D dunes and bars. Planar cross-stratified sandstones (Facies LF 4) were formed as 2-D dunes. The dominance of coarse and ungraded beds, low paleocurrent variability and rarity of lateral accretion surfaces indicates transportation by

Table 1
Lithofacies of the Matasiete and Pozo D-129 Fms in the San Bernardo Fold Belt

Lithofacies and sedimentary features	Interpretation
Fluvial facies	
LF1. *Matrix supported, cobble to pebble conglomerate*: Poorly sorted, massive or crudely bedded, not imbricated, medium-to-fine gravel clasts in a matrix rich in coarse-to-medium tuffaceous sand. Volcanic clasts, moderately rounded, although occasional broken clasts are found. Maximum clast-size observed was 12 cm, but most range from 2 to 5 cm. Thickness less than 2 m, in gradational or sharp contact with other coarse-grained lithofacies.	Mass flow deposited from highly concentrated sediment flows.
LF2. *Clast supported, cobble to pebble conglomerate with horizontal bedding*: Moderately sorted, crudely bedded with clast imbrication. Weak grading, a few beds fine upward. Sub-angular to moderately rounded clasts, volcanic and pyroclastic. Could contain large trunks and bone remains. Maximum clast-size observed ~10 cm, thickness 0.2 to 1.5 m. Base frequently erosional, top locally gradational to finer lithologies.	Lag deposits or sieve deposits, the thicker beds represent amalgamation of longitudinal bedforms.
LF3. *Clast supported, trough cross-stratified, pebble conglomerate and sandstone*: Base commonly erosional, with fining-upward. Local mud intraclasts and dominance of volcanic clasts. Oriented wood fragments. Individual cross-sets are 0.2–1.8 m thick, separated by scour surfaces. Amalgamated bodies up to 7 m thick. Unimodal paleocurrents with generally low dispersion about the mean.	Downstream migration of 3-D dunes or oblique migration of longitudinal bars in channels.
LF4. *Clast supported planar–tabular stratified, pebble conglomerate and coarse sandstone:* Planar or scoured base, sets 0.3 to 0.9 m thick that fine upward and are in many cases amalgamated. Rare mudstone intraclasts and scarce wood fragments. Imbricated clasts and unimodal paleocurrent distributions.	Downstream migration of 2-D dunes or linguoid bars.
LF5. *Pebble conglomerate and coarse to medium sandstone with desiccation cracks*: This lithofacies occurs rarely on top of Facies LF3 or LF4. The cracks are polygonal to irregular in plan view, 2 to 4 cm deep, and are filled by dark, massive, more consolidated mudstone.	Abandoned channel with subaerial exposure.
LF6: *Fine to medium sandstone with asymmetrical ripples*: Rare. Thin beds (<0.3 m) overlying flat-based conglomerate bodies, associated with small-scale planar cross-lamination. Ripple sets are 0.01 to 0.03 m thick and 0.1 m in wavelength. Unimodal paleocurrents.	Downstream migration of ripples in lower flow regime.
LF7: *Coarse to fine sandstone with inclined large-scale surfaces*: Found in the Upper Member. Consists of bedsets 0.5 to 5 m thick, with low-angle basal surfaces (<10°), internally containing low-angle cross bedding and trough cross-bedding that fines upward. Finer lithologies locally show asymmetrical ripples. Palaeocurrents are near orthogonal to the strike of the inclined surface.	Lateral accretion deposits.
LF8: *Medium to fine sandstone with horizontal lamination.* Dm-scale packages of planar-laminated, fine-grained sandstones. Individual beds are ~1 cm thick and can be traced for several m, internally ungraded or fine upward. Some beds contain gravel.	Upper or lower flow regime plane beds.
LF9. *Tabular or lobate fine to medium sandstone*: Planar or erosional base, lenticular geometry; planar or convex-upward top, occasional pebbles and general fining-upward trend. Low-angle and trough cross-bedding; commonly interbedded with beds of Facies LF9. Thickness ranges from few tens of cm to 0.8 m thick.	Overbank deposition into crevasse channels, lobate deposits represents crevasse splay.
LF10. *Red to yellow–brown, massive to laminated siltstone and claystone*: Tabular geometry, beds are fine-laminated or massive, occasionally mottled. Locally contains abundant calcium carbonate nodules (caliche), as isolated, concentric nodules or thin, tabular beds, sparsely root-bioturbated. Occasionally pale-grey or white in color; contains small-scale symmetrical ripples and *Planolites, Palaeophycus* and *Taenidium* fossil traces.	Subaerial, distal floodplain deposits, soils with chemical precipitation. Occasional isolated, ephemeral, very shallow-water deposition.
Pyroclastic facies	
LF11: *Tabular fine-grained tuff with horizontal bedding*: Planar base, ungraded beds 0.3 to 3.5 m thick. Massive or horizontal stratified. Moderate to well sorted, subangular clasts, rare accidental lithic clasts. Mottling (local to pervasive) and root traces (vertical to subvertical, up to 10 cm long) on top of individual beds.	Pyroclastic deposits from volcanic ash fall-out. Incipient to full pedogenic modification.

(continued on next page)

Table 1 (*continued*)

Lithofacies and sedimentary features	Interpretation
Pyroclastic facies	
LF12: *Grey fine-grained tuff with low-angle cross-bedding and antidune bedding*: Tabular geometry, thickness up to 1 m, individual sets are less 0.15 m thick and 1.5 m wavelength, unwelded, with undulated base, pumice clasts, glass shards, and orientation of lithic clasts. Gradational contact between coarse and fine strata, containing low-angle cross stratification that laterally grades to plane-laminated beds. Dome like structures with low-angle cross-laminated beds dipping upstream and downstream.	Volcaniclastic flow (ground surge), upper and lower flow regime conditions. Turbulent flow.
LF13: *Grey fine-grained tuff with accretionary lapilli*: Plane or undulated base, ungraded beds 0.2 to 0.4 m thick. Massive, locally contains parallel lamination and rarely low-angle cross-bedding. Accretionary lapilli are up to 0.7 cm in diameter and exhibit concentric internal structure.	Volcaniclastic flow deposits. Deposition of accretionary lapilli from condensation into the pyroclastic surge or from ash-fall deposition.
LF14: *Grey horizontally laminated fine-grained tuffaceous sandstone*. Tabular geometry, consists of laterally continuous laminae or very thin beds internally massive; often associated to LF12. Common superposed sets with different laminae thickness.	Hyperconcentrated flood flow, possibly formed under rapidly aggrading conditions in super-critical flow conditions
Lacustrine facies (Pozo D-129 Fm)	
LF15: *Grey or blue–grey, tabular, oolitic limestone*: Planar or irregular base, amalgamated bodies up to 0.8 m in thickness, with concave-up tops. Internally massive or contain small-scale cross-bedding. Ooids form well sorted grainstones, their shape and size are spherical and about 2 mm in diameter, with no dolomite in their composition and diagenetic silicification.	Fresh-water limestone
LF16: *Grey or pale blue siltstone and claystone*: Planar base and tabular geometry, internally massive. Some thicker beds contain sand to silt laminae a few cm in thickness. Locally interbedded with white, tabular, fine-laminated or massive tuff. Scarce bioturbation and abundance of elongate carbonate nodules.	Alternating deposition from suspension and traction current in deep-lacustrine setting.
LF17: *Tabular, coarse to medium sandstone*: Planar or erosional base, and frequent concave-up top. Individual bodies are 0.3–0.6 m thick, moderately to well sorted, ungraded or fine-upward, amalgamated into packages c. 3.5 m thick. Tuffaceous clasts are dominant, but volcanic and rare limestone clasts present. Contains low-angle cross-bedding and occasional hummocky cross-bedding.	Bars and dunes deposited in a shallow lacustrine setting

high-energy currents and suggests the presence of low sinuosity, fixed channels (Bridge et al., 2000). The local occurrence of desiccation cracks on top of fining-upward in-channel strata records desiccation of surficial sediments between flood events (Collinson, 1996). Storeys displaying vertical reduction in grain size and internal structure, and preservation of rippled cross-strata (Facies LF6) on top indicate progressive reduction in discharge during filling, with slow and gradual abandonment of the channel. Avulsion was an important process in the infill of these channels. A few coarse-grained channels contain lateral accretion surfaces, which suggest helicoidal flow and lateral migration of these channels. Single storeys of these meandering channels are separated by laminated mudstones suggesting variable discharge and periods of inactivity. Convex-upward, large scale, inclined surfaces in tabular sandbodies suggest the diversion of the flow and presence of braided rivers.

3.1.3. Facies association 3: proximal floodplain

3.1.3.1. Description. This Facies Association (FA3) consists of small sandstone bodies less than 0.8 m thick (Facies LF9) encased in sparsely bioturbated reddish mudstones (Facies LF10) and occasional thin ash-fall beds (Facies LF11) with variable terrigenous clastic content, deposited adjacent to major sandbodies. The sandstone beds are mostly tabular, planar or erosionally-based and many contain red-coloured mudstone intraclasts. Internally they show low-angle and trough-cross bedding (Facies LF3) in sets up to a few tens of cm thick. Paleocurrent shows low dispersion in the measurements

and is mostly oriented at high angle to the adjacent, major sandbodies (Fig. 8). Many beds fine upward. Tops of sandstone beds are planar or concave-up, and typically gradational into Facies LF10. Coarsening or fining-upward trends are locally present in the interbedded sandstone and mudstone associations. This succession is commonly truncated by the presence of channel sandbodies. Where present, paleosols are dominated by thin

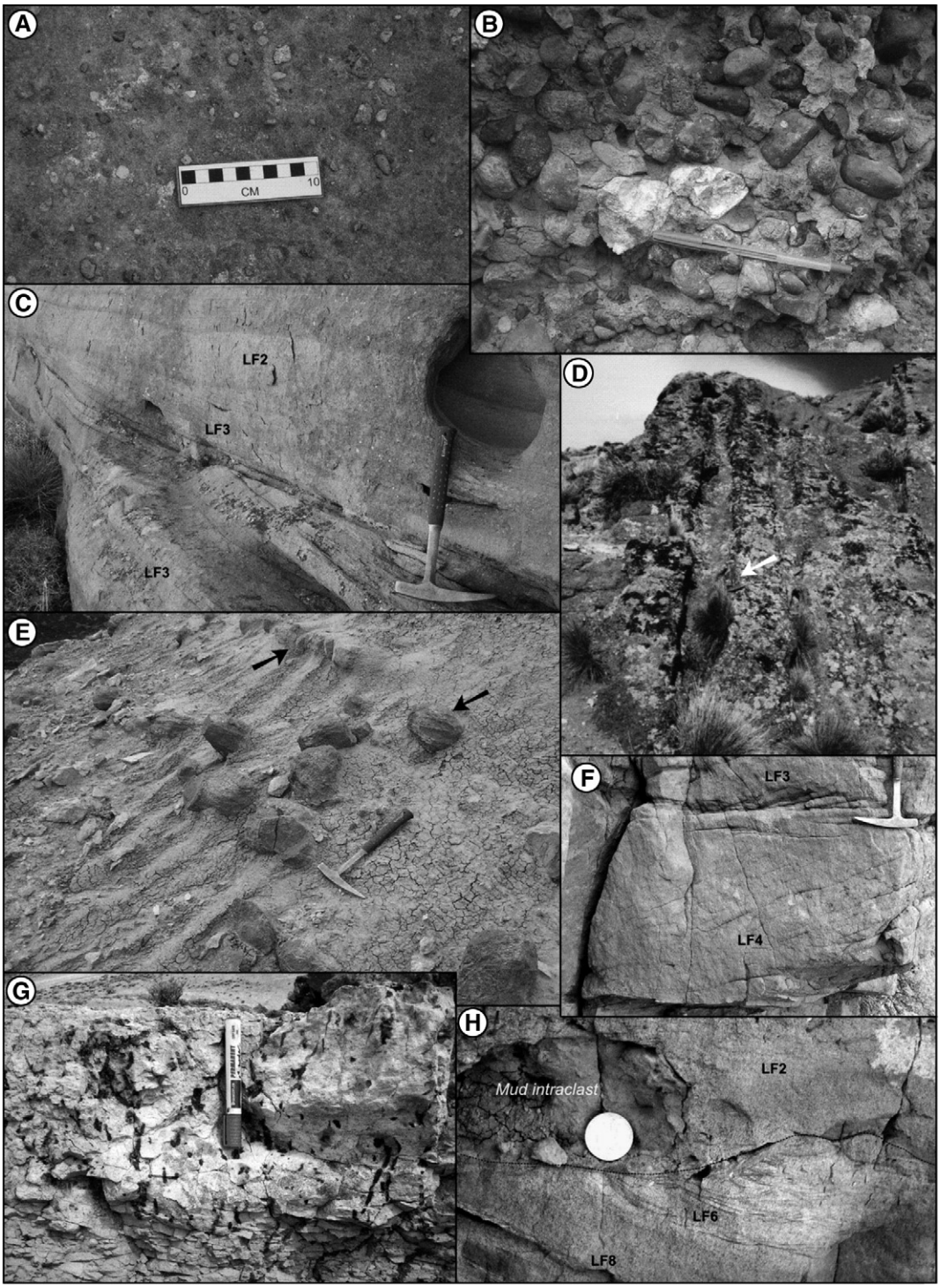

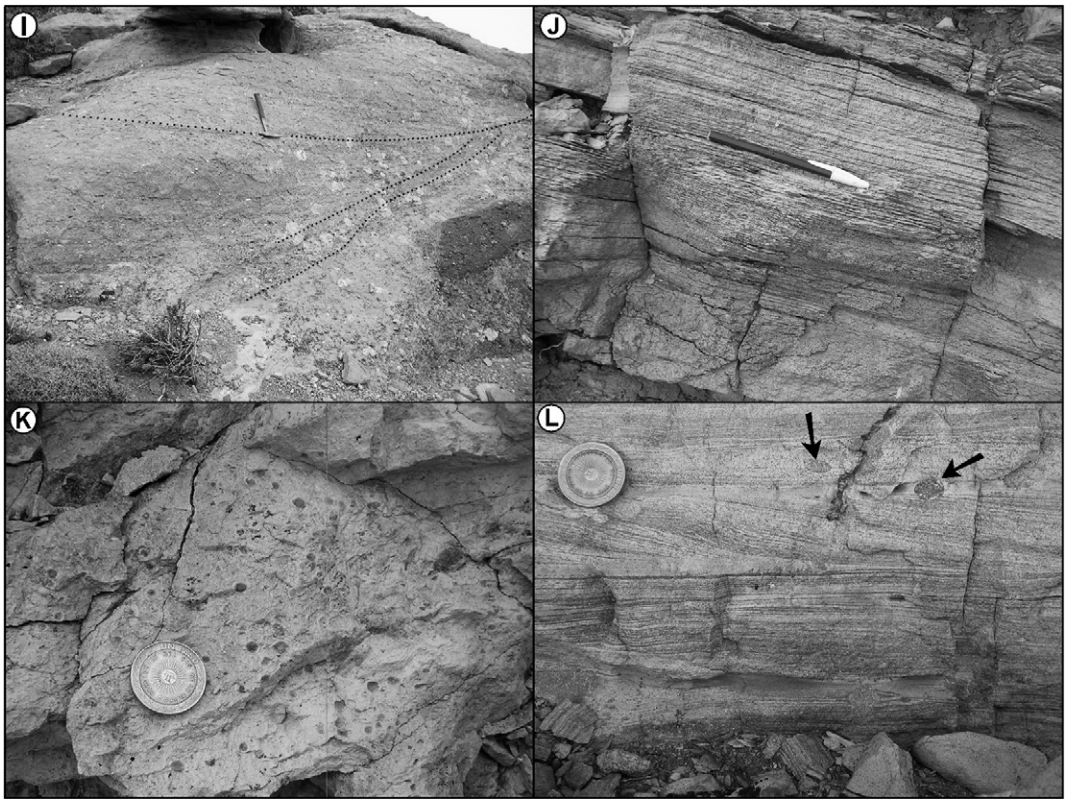

Fig. 6. Selected photographs of lithofacies. A) Matrix supported, fine gravels and sandstones (Facies LF1) preserved at the base of multistorey channels. B) Clast supported, fine gravel beds (Facies LF2). The gravels are moderately rounded, mostly dominated by acid volcanic clasts, ignimbrites and tuffs. Pen is 15 cm long. C) Planar–tabular fine gravels and sandstones (Facies LF4) over horizontally bedded sandstones (Facies LF2). D) Oriented trunks (voids) preserved in channel fill deposits. Lower Member of the Matasiete formation in the Matasiete Canyon. The arrow points to a hammer 0.3 m long. Trunks shown are up to 0.5 m in diameter and 15 m long. E) Fine distal floodplain deposits (Facies LF10) containing abundant, rounded, carbonaceous concretions (arrows). F) Coarse sandstone bed with planar cross-bedding (Facies LF4). G) Rooted white tuff (Facies LF10). Bioturbation increases towards the top, while the base contains parallel lamination. Scale in centimetres. H) Ripple cross-lamination (Facies LF6) preserved on top of a fining-upward bed. Sandstone over the erosive surface contains mud intraclasts (arrow). Coin is 15 mm in diameter. I) Amalgamated, meter-scale cross-bedded sandstones (Facies LF3). Paleoflow is to the upper right. Hammer is 0.3 m long. J) Fine laminated tuff (Facies LF14) at the base of a volcaniclastic surge deposit. K) Massive tuff containing accretionary lapilli (Facies LF13). L) Tuffs containing low-angle cross bedding (Facies LF12) are part of the surge deposits. Arrows mark post-event bioturbation tubes.

horizons of pedogenic carbonate and small rhizoliths (*sensu* Kraus and Hasiotis, 2006) preserved in fine sandstones.

3.1.3.2. Interpretation. Based in the small scale of their features, the sandstones represent crevasse splays and small crevasse channels, formed during high-discharge flood events in areas proximal to LA2 (Miall, 1996), with paleocurrents oriented at high angle to those of the adjacent channel fills. Coarsening-upward trends are indicative of successive flows arriving on a low-energy floodplain (Smith et al., 1989). Fining-upward trends are attributed to an increase in the distance to active channel belts or to the gradual reduction of the discharge. The return to suspension fallout is marked by deposition of mudstones or tuffs with paleosol horizons. Truncation of coarsening upward facies trend suggests avulsion via crevasse splay progradation of the main channel (Slingerland and Smith, 2004).

3.1.4. Facies association 4: distal floodplain

3.1.4.1. Description. This facies association (FA4) is dominated by reddish, massive to laminated claystones and siltstones (Facies LF10), and tabular beds of fine-grained tuff (Facies LF11). The association reaches a thickness of several tens of meters, and the main characteristics are the abundant carbonate concretions in the form of isolated, concentric nodules up to 0.4 m in diameter, or occurring as tabular and more consolidated beds. Pedogenic features are vertical root traces, mottling, slickensides and coalesced carbonate nodules (see

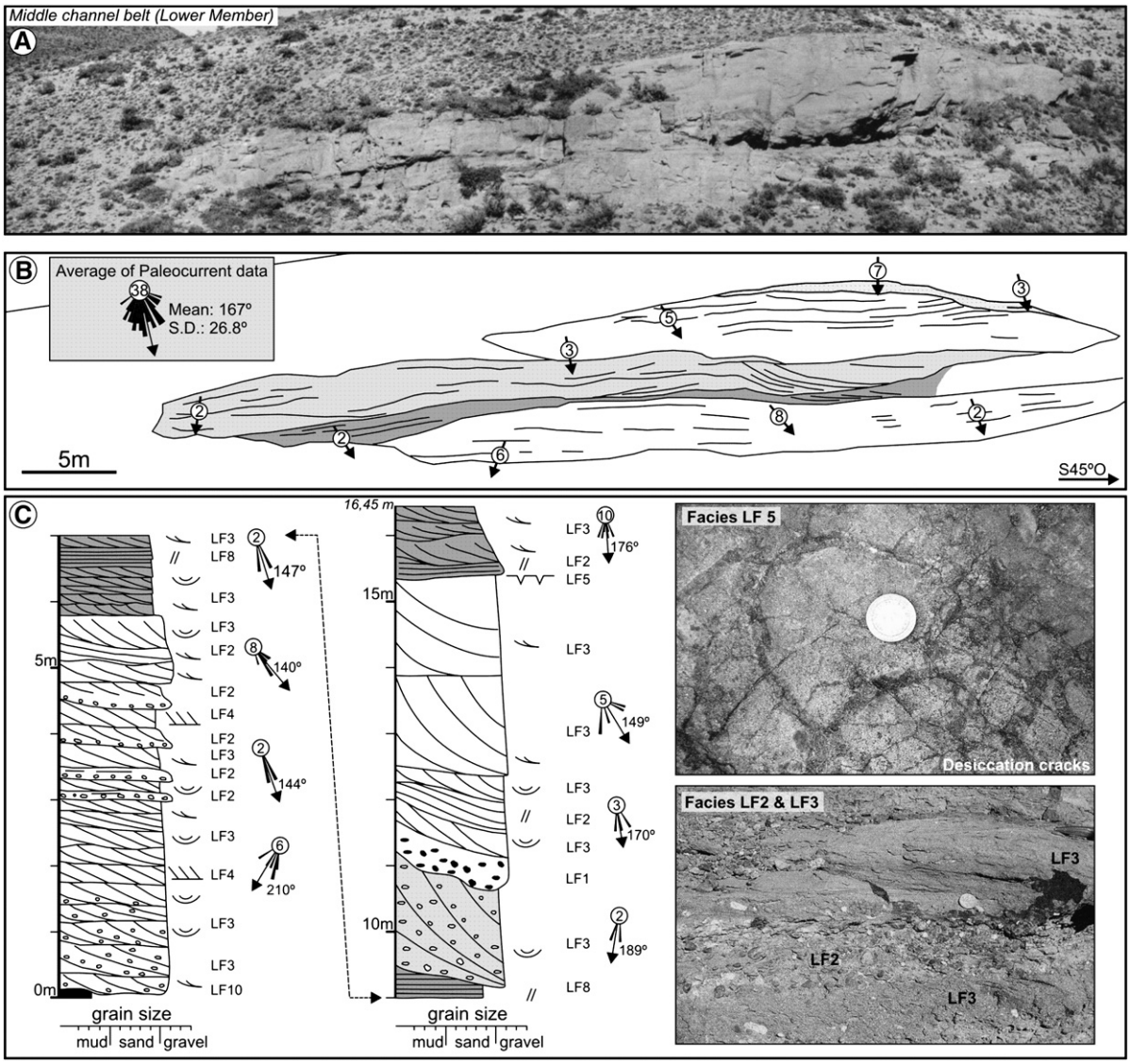

Fig. 7. Details of the multistorey channels. A) Photomosaic of a selected fixed, straight, multistorey sandbody, Lower Member in Matasiete Canyon B) Interpretation and distribution of paleocurrent data. C) Measured section of the multistorey sandbody and lithofacies details.

below). Trace fossils are common on bed surfaces or within beds, in the form of vertical, cylindrical, unlined and passively filled tubes. Some tabular, laminated fine-grained sandstone beds contain symmetrical ripples at their tops, as well as horizontal, multidirectional, meniscate burrows. The bioturbation intensity of most beds increases upwards, and pervasive bioturbation is common in some localities (Bellosi et al., 2002). In the upper Member, superimposed cycles grade upward from thick, yellow–brown coloured mudstone beds to red mudstone beds.

3.1.4.2. Interpretation. The red colour of most of this LA indicates subaerial exposure. The abundance of carbonate nodules indicates an excess of alkaline solutes and precipitation due to fluctuations in ground-water table in a well-drained floodplain (Retallack, 1988). Mottling results from periodic waterlogging (Wright, 1999). The presence of beds containing wave ripples and burrows (faunal feeding and/or dwelling activity) near the top suggests that deposition took place in very shallow-water or isolated ephemeral ponds (Abdul Aziz et al., 2003).

3.1.5. Facies association 5: pyroclastic deposits

3.1.5.1. Description. This facies association (FA5) consists of tabular, pale-grey or white, lithic-free tuffs (Facies

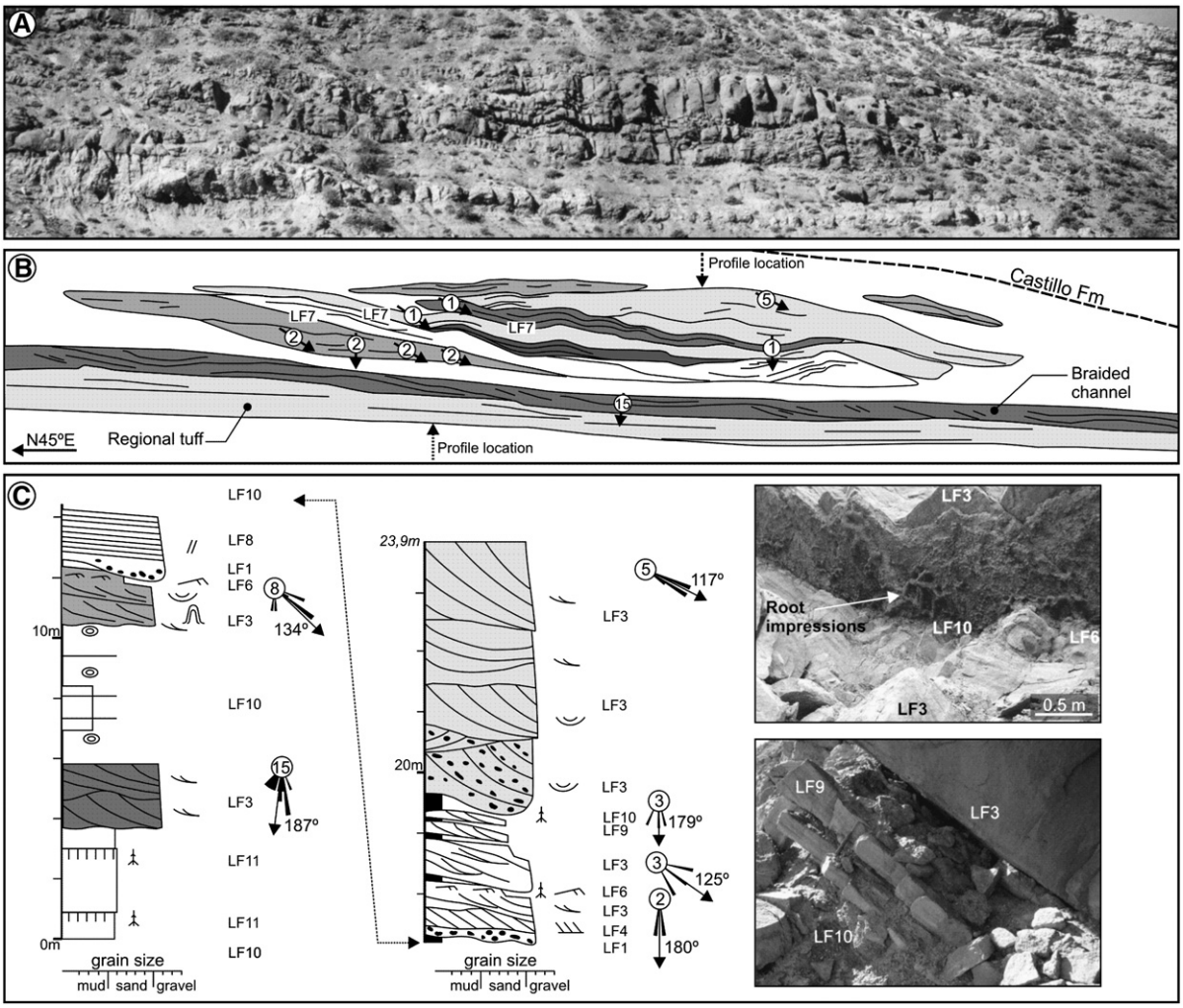

Fig. 8. Multistorey meandering fluvial channel from Upper Member in Matasiete Canyon (location in Fig. 5). A, B) Photomosaic and interpretation of the sandbody. Facies LF7 represent large-scale inclined surfaces that separated single episodes of infill of the channel. A braided channel is present on top of the white, tabular tuff shown in the lower part of the picture. C) Measured section and paleocurrent data. Pictures show details of sandstone lobes preserved in the margin of the channel and root impressions at the base of the channel. Hammer is 0.3 m long.

LF11), preserved in the three Members of the Matasiete Fm. The pyroclastic beds consist mainly of zeolite/smectite-replaced cuspate pumice shards, with sparse crystals of plagioclase and quartz. The tuffs are massive or finely laminated and frequently show root traces and vertical to horizontal burrows on top. Two beds identified towards the top of the Middle Member in the Matasiete Canyon (Fig. 9) are about 4.5 km in lateral extent and 1 to 3 m thick and show the vertical stacking of plane-based, fine laminated tuffs (Facies LF14) containing accretionary lapilli (Facies LF13), followed by several dm-thick beds of low-angle cross-bedded and finely laminated tuffs, which tend to thicken within gentle depressions and thin over crests of undulations (Facies LF12). Accretionary lapilli are in many places concentrated into thin strata. Near-symmetrical bedforms are thin (<0.15 m thick) with wavelengths of about 0.7 to 1.5 m, and internal laminations dipping downstream and upstream. Individual beds are ungraded, but the general trend is coarsening-upward owing to the presence of accidental tuffaceous clasts in the upper sets. Occasional elongate biotite grains are displayed parallel to the base of the bedforms.

3.1.5.2. Interpretation. The deposition of fine, massive tuffs with root traces or burrows was formed by intermittent deposition of ash-fall as tabular beds in low-gradient, subaerial and subaqueous areas of floodplains (Cas and Wright, 1987). Tuff beds containing asymmetrical ripples and small-scale cross-bedding indicate transportation by turbulent flows in lower flow regime

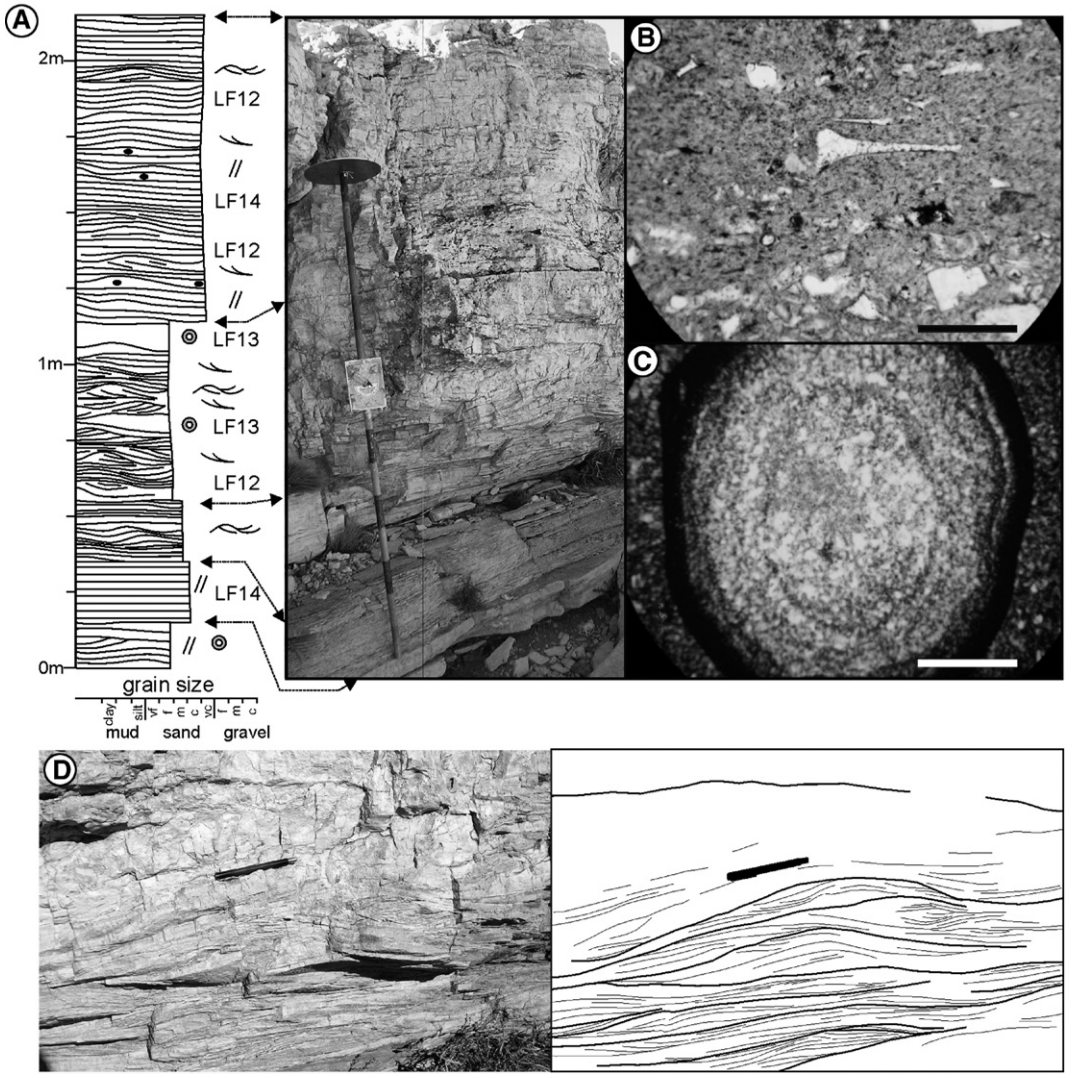

Fig. 9. A) Stratigraphic section of ground-surge deposits in uppermost part of Middle Member at Matasiete Canyon (location in Fig. 5). B) Photomicrograph of finely laminated tuff (Facies LF12) with cuspate Y-shaped shards and plagioclase fragments (arrow). Scale bar is 0.5 mm. C) Photomicrograph of accretionary lapilli, rim-type, from the basal section of the pyroclastic surge. The coarse-grained core is coated by at least seven layers of progressively finer-grained, darker, ash. Scale bar is 1 mm. D, E) Outcrop view and sketch of dome-like forms interpreted as antidune structures (Facies LF12) interbedded with low-angle cross-stratified tuffs. Pen is 14 cm long. Flow is from left to right.

condition. The dome-like structures with sets of laminae dipping upstream and downstream are interpreted as antidune structures (Alexander et al., 2001).

The extensive, tuffaceous beds containing low-angle cross bedding and horizontal lamination and rare antidune bedding indicates transportation by flows that are transitional from the upper plane bed to antidune stability fields (Fielding, 2006). These beds indicate the presence of ground-surge deposits associated with contemporary volcanic events (Fisher and Schmincke, 1984; Carey, 1991; Schumacher and Schmincke, 1995).

3.2. Facies associations of the Pozo D-129 formation

3.2.1. Facies association 6: shallow lacustrine environment

3.2.1.1. Description. The shallow lacustrine association (FA6) consists of tabular oolitic limestone beds (Facies LF15) and low-angle cross-bedded and hummocky cross-stratified coarse to fine sandstone beds (Facies LF17). Some clastic beds display erosional bases and fining-upward trends, but others have a planar

base and concave-upward top, and show partial superposition of lenses about 1 m thick and few tens of meters width. Many beds contain oolitic limestone clasts as part of a basal lag. The carbonate lithofacies comprise oolitic grainstones without dolomite. The ooids are regularly shaped, show several concentric laminae, and do not contain detrital components (Fig. 10B). Their nuclei often consist of microfossils.

3.2.1.2. Interpretation. The presence of basal erosional surfaces, fining-upward trends and moderately-to-well-sorted sandstone beds, plus the presence of sedimentary structures generated in a lower flow regime, suggest in-channel deposition from turbulent flows. Hummocky cross-bedding is evidence of oscillatory and multidirectional flows, related to storm waves. The occasional presence of partially superposed, lobate beds indicates unconfined deposition in bar complexes. Both facies may be preserved in a low-gradient marginal lacustrine setting (Link and Osborne, 1978). The oolitic grainstone beds require a well-oxygenated shallow-water body and excess of alkaline solutions for their formation. Such conditions are met during intervals of reduced sediment supply, and in areas sheltered from clastic input (Talbot and Allen, 1996).

3.2.2. Facies association 7: deep-lacustrine environment

3.2.2.1. Description. This facies association (FA7) is recorded in outcrops exposed to the south of the Matasiete Canyon, Silva Hill and Codo del Senguerr anticline (Locations 1, 2 and 4 in Fig. 1). It mostly consists of grey or pale blue, poorly consolidated, locally bioturbated but more commonly fine-laminated claystones and siltstones (Facies LF16) and thin tuff beds (Facies LF11). Thin, lenticular, fine sandstone beds containing ooids and abundant carbonate nodules a few cm in diameter are occasionally intercalated in these laminated beds. In southern areas (e.g. Codo del Senguerr), FA7 is dominated by stacking of white, massive or finely laminated tuffs.

3.2.2.2. Interpretation. A low-energy environment is inferred from the dominance of extensive, finely laminated deposits. The calcareous composition of the nodules indicates saline–alkaline waters and oxidizing conditions (Platt and Wright, 1991). The absence of any preserved evaporite facies suggests an abundant supply of fresh water to the lake, which prevented evaporation and concentration of salts (Talbot and Allen, 1996). The associated tuff beds indicate spasmodic volcanic activity

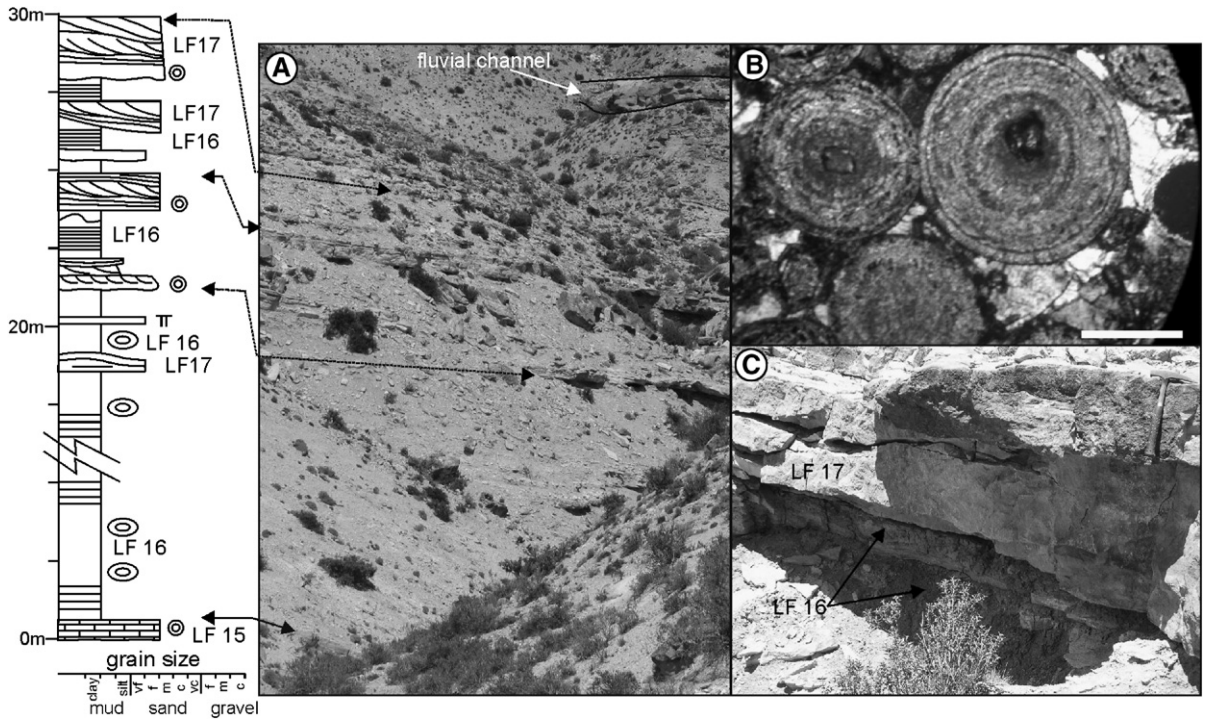

Fig. 10. A) Stratigraphic section of the lacustrine Pozo D-129 Fm in Chenque (Silva) Hill. B) Photomicrograph of well-rounded oolitic grainstones (Facies LF15). Scale bar is 1 mm. C) Grey mudstones (Facies LF16) and amalgamated sandstone beds (Facies LF17) preserved in a shallow lacustrine environment.

in the hinterland and slow deposition under subaqueous conditions.

4. Fluvial architecture

Good exposures of the channelized deposits in the Matasiete Canyon, architectural diagrams and detailed measurements of stratigraphic profiles were used to reconstruct the fluvial architecture. The coarse fill of channels and the rarity of lateral accretion surfaces (observed in only 2 out of 100 channels) permitted the real width of each channel to be obtained from its apparent width and the direction normal to paleoflow. A compilation of the paleocurrent measurements obtained from the unit is presented as Fig. 11. In this way, measurements of channel width/thickness ratios (hereafter abbreviated as W/T ratios) were obtained (Fig. 5) for each of the three Members in the Matasiete Canyon and compared to the channel classifications developed by Friend (1983) and Friend et al. (1979). Most of the single or multistorey fluvial channels of the Matasiete Fm could be described as "sandstone ribbons" using the criterion ($W/T<15$) of Friend et al. (1979). Despite the large lateral extent of some of the sandbodies, no sheets with $W/T>100$ were identified (see Fig. 12).

4.1. Lower Member

This Member is exposed in the Matasiete Canyon only, where most of the multistorey sandbodies have a W/T ratio <10. In the uppermost sandbodies the W/T ratio reaches 35.6 (W/T values range from 2.3 to 35.6). Multistorey channels of the Lower Member have an average thickness of 7.2 m (range 2.0 to 16.5 m) and an average width of 47 m (range 20 to 162 m). The proportion of channels in two measured sections at Matasiete Canyon is 27% and 38%. Three main channel belts, separated by floodplain deposits, are present in the most sand-rich section of this Member. Paleocurrent directions within each belt are variable (see Fig. 11), but dispersion of measurements in single channels is low. The basal channel belt flows to the northeast (vector mean = 64°, standard deviation = 21°, $n=89$), the middle one to the southeast (mean = 174°, SD = 21°, $n=24$), and the upper belt to the east-southeast (mean = 110°, SD = 31°, $n=63$). Channel sandbodies lack lateral accretion surfaces, show multiple erosional surfaces, low variability in the paleoflow in single channels, and frequent fining-upward trend. This evidence suggests that avulsion was an important mechanism for migration of these fixed, coarse-grained channels. The presence of desiccation cracks on top of some amalgamated sandstone beds suggests complete desiccation of the channel bed after avulsion or abandonment, and exposure of in-channel dunes and bars.

4.2. Middle Member

This Member is exposed in the Matasiete Canyon only. The deposits reflect a dominance of floodplain

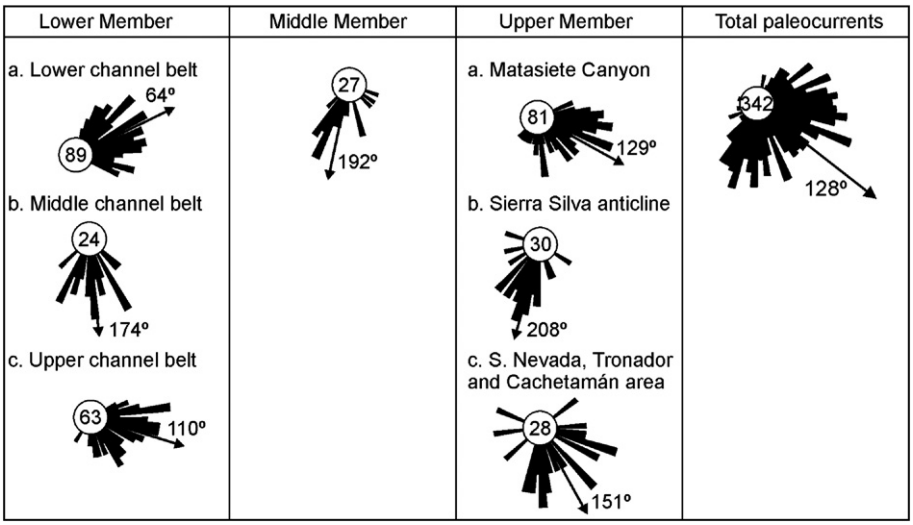

Fig. 11. Rose diagrams showing the distribution of mean paleoflow in the three members of the Matasiete Formation. Data from the Lower Member at the Matasiete Canyon are separated by channel belts. Data from the Middle and Upper Member in the Matasiete Canyon and Sierra Silva are mainly parallel to the major fault of the basin. Data from the remainder areas (e.g. Sierra Nevada, Tronador and Cachetaman area) are scarce, but show a quite similar paleoflow direction.

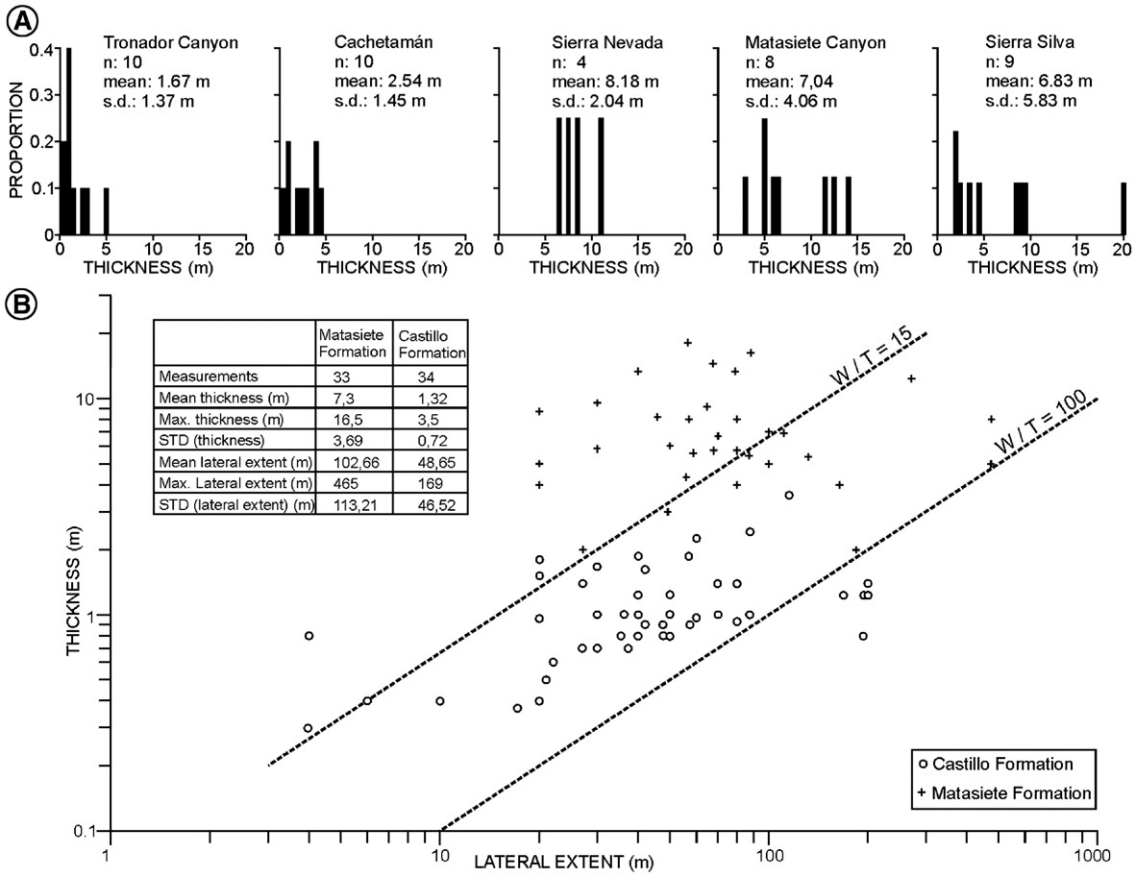

Fig. 12. A) Thickness variation, mean and standard deviation data from the Upper Member of the Matasiete Formation at several locations. B) *W*/*T* ratio of fluvial sandbodies of the Matasiete and Castillo formations at Matasiete Canyon. The data reflect a reduction of sediment supply during the deposition of the Castillo Formation and changes in the geometries of the sandbodies.

fines over channelized facies, the latter comprising 15% and 24% of the total thickness of two measured sections. Sandbodies in the Middle Member have an average thickness of 6.5 m (range 2 to 11 m) and an average width of 134 m (range 65 to 450 m). The channels are not connected and reflect transportation to the south (vector mean = 192°, SD = 27°, n = 27). The *W*/*T* ratio is laterally variable (Fig. 5), but increases toward the top of the Member (range 14.5 to 75). The largest *W*/*T* ratio (75) is recorded on top of the extensive volcaniclastic beds shown in Fig. 9.

4.3. Upper Member

The architecture of the Upper Member is similar to that of the Middle Member, with isolated multistorey sandbodies encased in thick floodplain deposits. Multistorey channels make up 21% and 26% in two measured sections at Matasiete Canyon, 30% in the Chenque (Silva) Hill, 28% in the Cachetamán area, 16% in the Sierra Nevada anticline, and 11% in the Tronador section. Channel thicknesses and their standard deviations are presented in Fig. 12A. The average thickness of the channels in the Upper Member at Matasiete Canyon is 7.0 m (range from 2 to 14.4 m in Matasiete Canyon, one sandbody of 20 m thick in Silva Hill) and the average width equals 126 m (range from 50 to 440 m). The mean paleotransport direction is south-southeast in the Matasiete Canyon and Sierra Silva anticline (mean = 168°, SD = 46°, n = 111) but individual sandbodies show variations of 80° to 100° around the mean. The *W*/*T* ratio of the multistorey channels is less than 20 (see Fig. 5), except in a unique sandbody characterized by a *W*/*T* ratio of 90. This sandbody is a homogeneous, coarse-grained bed, directly overlying a white, tabular, 3.5 m thick tuff bed. In the core of the Sierra Nevada anticline the exposures of the Upper Member of the Matasiete Fm (Sciutto and Martínez, 1996) show an average channel thickness of 8.2 m (n = 4), comparable to the sandbodies in the Matasiete Canyon. Exposures

of the Upper Member in the Tronador Canyon and Cachetamán Hill are characterized by channels with an average thickness of 1.6 m ($n=10$) and 2.5 m ($n=10$), respectively. The small size of these channels suggests that these outcrops represent deposits of a less integrated fluvial system or, alternatively, they could be part of a tributary system draining to the southern areas (e.g. Sierra Nevada, Matasiete and Sierra Silva), where the scale of the sandbodies is about 4 times greater.

4.4. Architecture of the Matasiete and Castillo Fms

Differences in thickness and W/T ratio of the Matasiete and Castillo Formation are shown in Fig. 12B, which is based on measurements at Matasiete Canyon. The data reflect a reduction in thickness of sandbodies in the Castillo Formation relative to those below and a general change in channel shape from ribbons ($W/T<15$) in the Matasiete Formation to sheets ($W/T>15$) in the Castillo Formation. These data support the hypothesis that sediment supply decreased during deposition of the Castillo Formation (Hechem and Strelkov, 2002), but further studies are needed to clearly understand the role of the ash-dominated floodplain and other controls (vegetation, discharge, changing paleogeography at the basin margins) on the behavior of the fluvial systems of the Castillo Formation, which is beyond the scope of this contribution.

5. Paleosols

More than 70% of the sections of the Matasiete Fm consist of mudstone and siltstone, and frequently the quality of the exposures is poor. The Upper Member was examined at Matasiete Canyon, where a detailed analysis of a representative section (20 m thick) was carried out. Yellow–brown and red siltstone–claystone beds are the dominant lithologies in the studied section (Fig. 13). Smectite and analcime are the dominant components in the <2 μm size fraction, and low proportions of illite are present in two samples. Red and yellow–brown mudstones frequently have a blocky or prismatic texture (>20 mm), although the yellow–brown strata show a finer blocky texture (<10 mm). Carbonate concretions form discrete nodules ranging from 5 to 40 cm in diameter, or rods of 10 to 25 cm in diameter and 100 to 150 cm length. Locally, coalescent rods and nodules are found (Stage I, II and III *sensu* Machette, 1985). Yellow–brown mudstones contain slickensides, which are found as clay-lined fractures that intersect to form concave-up, dish-shaped structures. On the top of some soil profiles (A horizon) there are desiccation cracks to 0.25 m deep, filled by a mixture of unsorted sandstone and mudstone or laminated beds. Rhizoliths (Klappa, 1980; Kraus and Hasiotis, 2006) a few millimeters in diameter are common both in the red and the yellow–brown beds. Elongate, light-grey rims (mottling) with circular cross-sections are common; they represent "drab haloes" (locally reduced zones) around root traces (Retallack, 1990). XRD analyses showed that the red to yellow–brown colour reflects the relative proportions of hematite (Fe_2O_3) and goethite (FeO(OH)), respectively (Cornell and Schwertmann, 2003). One sample contains jarosite ($KFe_3(SO_4)_2(OH)_6$). The paleosols record well-developed stress features (e.g. pseudo-anticlines, well developed blocky or prismatic ped structure and deep desiccation cracks) typically associated with intense expansion and contraction (FitzPatrick, 1980; Birkeland, 1984), features frequently attributed to vertisols (Marriot and Wright, 1993). The common occurrence of well-developed carbonate rods and nodules also indicates low sedimentation rates and seasonal oscillation of the water table (Allen, 1986; Marriot and Wright, 1993). These observations support the semiarid climate conditions suggested by Hechem et al. (1987) based on microfossils in the time-equivalent lacustrine Pozo D-129 Fm. Paleosols developed on pyroclastic strata only show vertical root traces and burrows attributed to *Planolites*, *Skolithos* and rare *Taenidium*; these incipient paleosols without horizons were interpreted as inceptisols.

6. Fluvial styles

The inferred depositional processes, facies and lithofacies associations, as well as architecture and paleocurrents of the Matasiete Fm, have been used to interpret the evolution of fluvial styles within the units. The application of discrete classification schemes to fluvial systems is problematic because they are based on different properties, and aim at simplifying the continuum of natural processes (Miall, 1996). The well-known subdivision into straight and meandering rivers is based on sinuosity. Other classification schemes are based on sinuosity and sediment type (Schumm, 1963, 1977), floodplain behaviour (Nanson and Croke, 1992) or channel style (Woolfe and Balzary, 1996). Our approach to the analysis of fluvial architecture is based on channel planform and rates of channel migration relative to floodplain aggradation rate.

Interpretation of fluvial style was based on the presence of: (a) coarse-grained infill of many of the sandbodies; (b) ribbon geometries of most of the sandbodies;

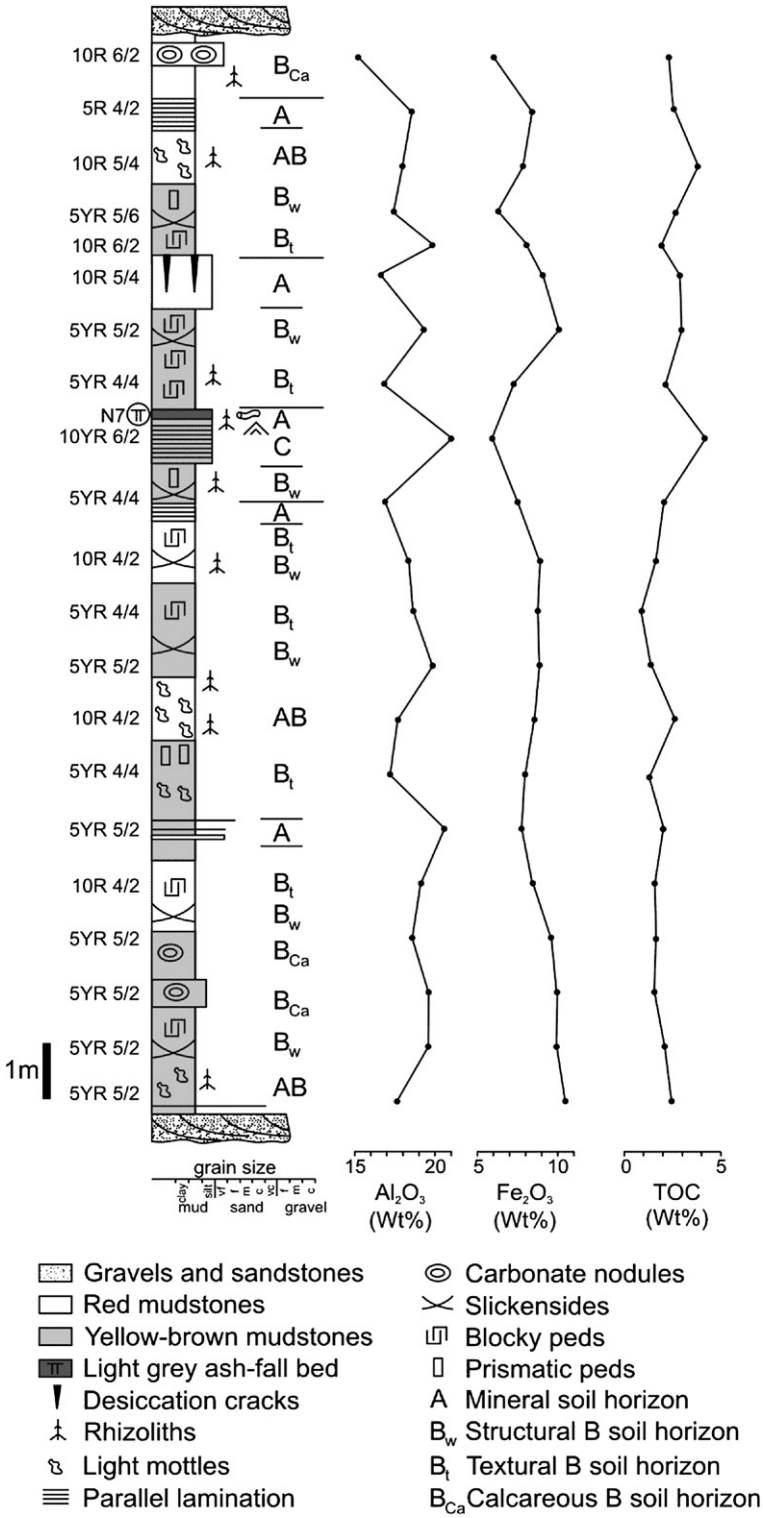

Fig. 13. Stratigraphic and chemical data for fine-grained rocks from the Upper Member at Matasiete Canyon (location in Fig. 5).

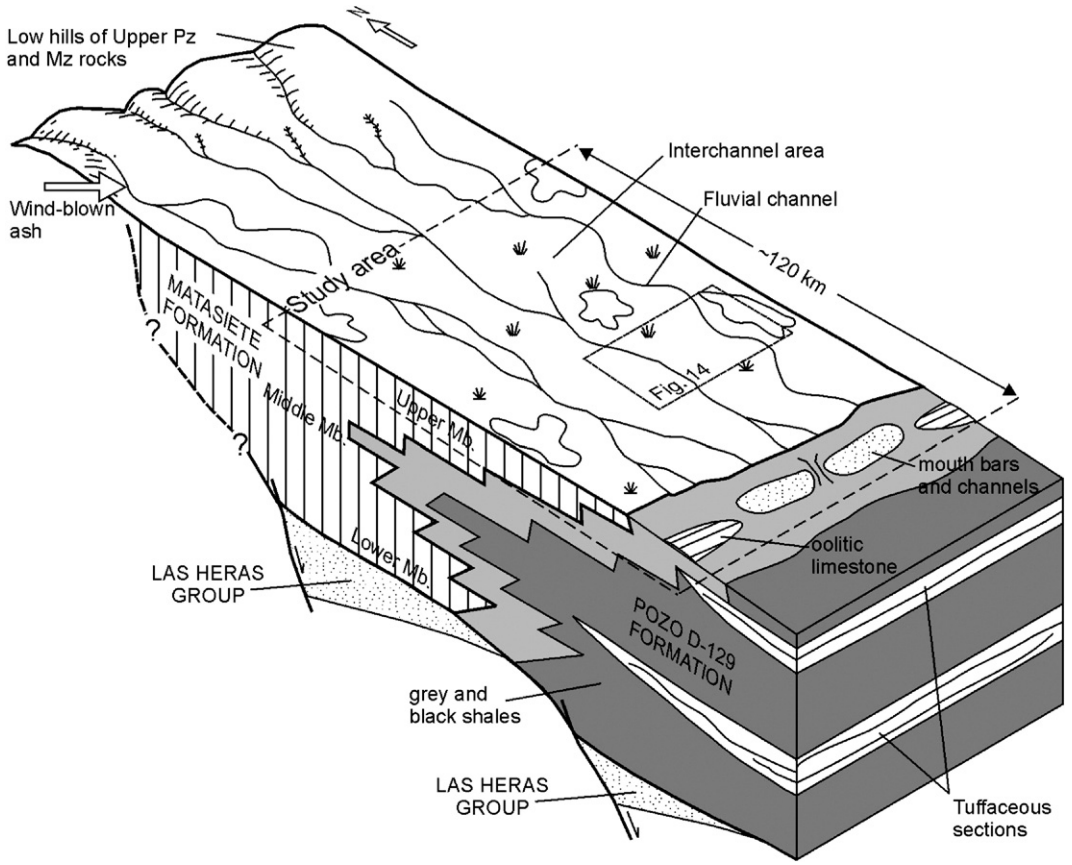

Fig. 14. Schematic environmental reconstruction for continental deposits of the Matasiete and Pozo D-129 formations. Vertical scale is greatly exaggerated.

(c) low dispersion in paleocurrent vectors in single channels; (d) stories displaying vertical reduction in grain size and internal structure, and preservation of rippled cross-strata in the upper parts; (e) scarce sandbodies containing lateral accretion bedding; (f) laminated mudstones on top of fining-upward trends related to lateral accretion bedding in multistorey meandering channels; (g) rare desiccation cracks on top of single channels; (h) oriented tree trunks of ~ 1 m in diameter along channel margins, likely incorporated as bedload; (i) high, but variable, mudstone to sandstone ratio, and (j) vertisols in the distal floodplain, which contain desiccation cracks, slickensides and carbonate nodules.

Most of the above features indicate that transportation occurred primarily during high-discharge flood events, with evidence of gradual abandonment in some multistorey channels. The paucity of deep incisions and the preservation of interchannel deposits indicate that aggradation rates in the channel belts exceeded those of the floodplain. Most of the studied sandbodies correspond to Field 1 of Woolfe and Balzary (1996).

The proportion of sandbodies in several sections from the three Members varies from 11% to 38%. Up to 80% of the channels analyzed in the seven studied areas are coarse-grained, lenticular, lack lateral accretion surfaces and display low dispersion of paleoflow measurements (<50°). We consider these sandbodies to be straight (Rust, 1978). The presence of large oriented trunks located at the margins of these channels suggests that riverbanks were vegetated. A few channels contain epsilon cross-stratification and lateral accretion surfaces, have a fining-upward trend and display a considerable variation in paleoflow measurements (~ 80–100° around the vector mean), indicating the presence of helicoidal flow patterns and meandering behaviour (Miall, 1996). It should be noted that such features could have been produced in meandering or braided rivers (Allen, 1983; Bristow, 1987). Single episodes of lateral migration are separated from each other by pale-grey laminated mudstones several tens of centimeters thick, suggesting that channel beds were periodically inactive. A few channels are filled by cobble to pebble conglomerates,

have high *W*/*T* ratio (>50) and are volumetrically dominated by the stacking of in-channel dunes. These show very low dispersion in paleocurrents, and are regarded as braided rivers. This pattern developed on top of tabular, pyroclastic ash-fall deposits or pyroclastic surge deposits, which suggests that the modification from single channels to a multichannel system (braided) was strongly controlled by substrate characteristics, and bears no relation to base-level changes.

The fluvial systems of the Matasiete Fm were previously interpreted as meandering (Sciutto, 1981) and braided to meandering (Galeazzi, 1989), while changes in fluvial style were attributed to base-level changes. Paredes et al. (2003, 2004) also favoured an interpretation in terms of braided and meandering fluvial styles, but pointed out that many multistorey channel fills did not fit into this classification. The presence of straight, meandering and braided channels in the Matasiete Fm suggests that different reaches of the fluvial system have had a different pattern along their course.

Both anastomosing rivers (Nadon, 1994; Makaske, 2001) and anabranching rivers (Nanson and Knighton, 1996; Tooth and Nanson, 1999) share many sedimentological attributes with the Matasiete Fm, notably the large proportion of overbank and floodplain deposits, the presence of straight, meandering and braided channels, the predominance of ribbon-like geometries and the poorly developed upward-fining trends in many channels fills. We believe that a hybrid model better represents the complex features observed in this gravel-dominated fluvial system (Fig. 14), but the occurrence of the Matasiete Fm in the core of anticlines, with few three-dimensional exposures, and the impossibility of proving that individual channel-fills were formed by coeval active channels make doubtful the categorization of the unit into one of these fluvial styles.

7. Discussion: external controls on sedimentation

7.1. Tectonism

The increase in accommodation during deposition of the lacustrine facies of the Pozo D-129 Fm (Barremian?–Aptian) is considered to be related to extensional or transtensional tectonics (Figari et al., 1999). Evidence includes rapid thickness variation and facies changes in the subsurface of the basin. The original tectonic relationships are obscured in the outcrops of the Pozo D-129-Matasiete depositional system along the San Bernardo Fold Belt, because of the strong tectonic inversion and extensive flood basalts covering the landscape (see Fig. 1C). The only indirect evidence of tectonic control on sedimentation is the near-orthogonal pattern of paleocurrent directions recorded between three consecutive channel belts of the Lower Member (Fig. 11), which indicate an alternation of transportation to the NE (64°), S (174°) and E-SE (110°). These changes could be related to nodal avulsions, or represent the entry of fluvial systems transversal and longitudinal to the NNW-SSE oriented ancient normal faults. The Middle and Upper Members show a consistent paleoflow direction to the south at Matasiete Canyon and Sierra Silva (Middle Member=192°; Upper Member=168°), broadly parallel to the tectonic structure.

7.2. Base-level changes and depositional sequences

Galeazzi (1989) considered the Lower and Middle Member as part of a unique depositional sequence, and located the sequence boundary at the base of the channels that cover the volcaniclastic beds in the topmost part of the Middle Member. The Upper Member was considered to be part of a second depositional sequence. By contrast, Hechem et al. (1990) considered the Lower Member as a single depositional sequence, and included the Middle and Upper Members in a second depositional sequence. The Middle Member was interpreted as a retrogradational system and the Upper Member as a progradational system, both related to episodes of expansion and contraction of the lake. However, field evidence did not allow the recognition of sequence boundaries according to the criteria proposed by Leeder and Steward (1996) and Shanley and McCabe (1994).

Paredes et al. (2003) rejected the concept of base-level control on channel geometry, and instead noted a relationship between sandbody geometry and the occurrence of tabular pyroclastic beds in the Middle and Upper Members at Matasiete Canyon, which is unrelated to base level. There are no substantial changes in fluvial architecture (eg. mean thickness of the channels, *W*/*T* ratio, and sandstone/mudstone ratio) between the Middle Member (retrogradational sets) and Upper Member (progradational sets). Moreover, most of the sandbodies are located towards the upper part of the Upper Member (Fig. 5, see Fig. 14 in Paredes et al., 2003), which reflects a reduction in the rate of accommodation, or higher rates of avulsion in the uppermost Upper Member.

7.3. Climate

The climate during deposition of the Matasiete-Pozo D-129 system was deduced from the presence of *Classopolis* pollen, and the common occurrence of oolitic grainstones and *Botryococcus*-like algal forms in the

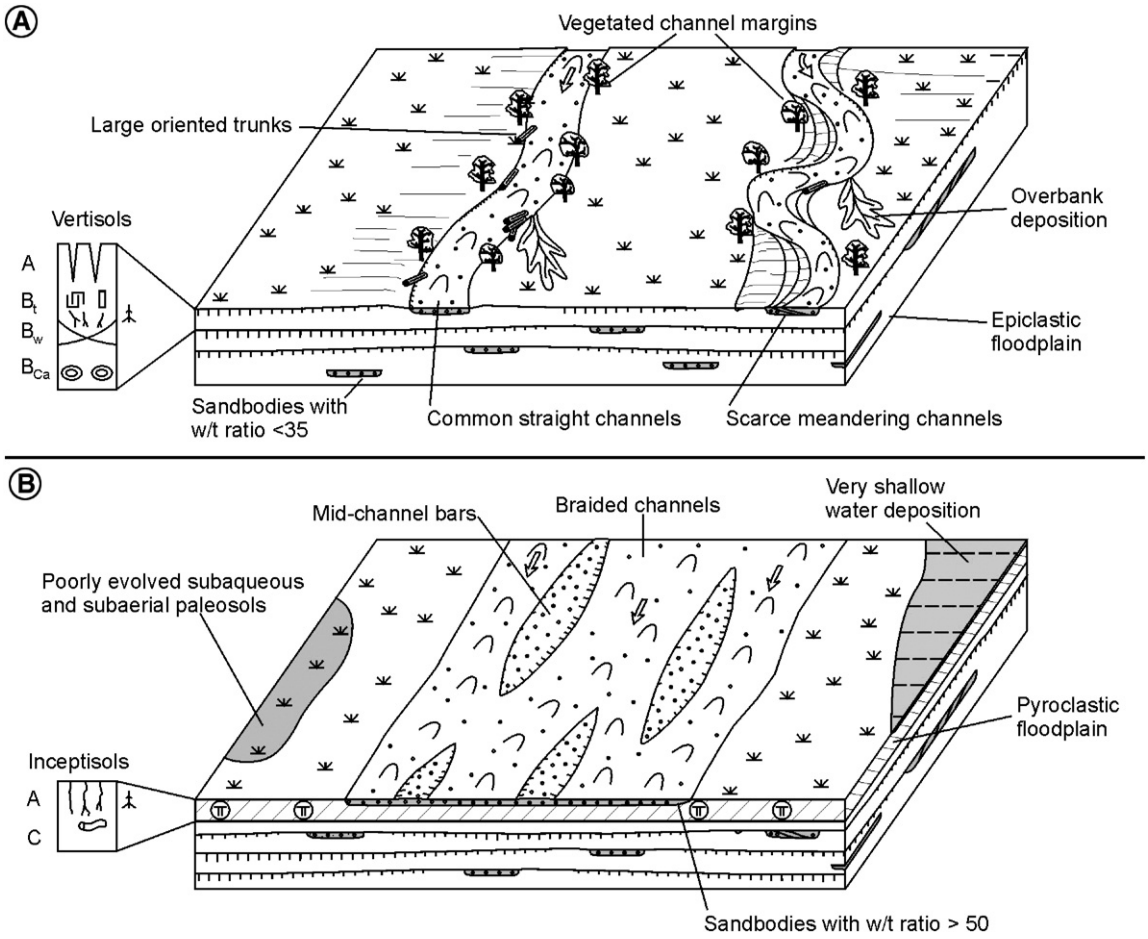

Fig. 15. Geometry of the fluvial sandbodies and their relation to the supply of pyroclastic material. A) Single or multistorey channels carved in an epiclastic floodplain show straight and rare meandering patterns. B) Channels are wider and display a braided pattern after pyroclastic supply events.

lacustrine facies (Hechem et al., 1987; Van Nieuwenhuise and Ormiston, 1989). These observations suggest a perennial and stratified saline–alkaline lacustrine system in a semiarid climate. Paleosols indicate a seasonal climate, as inferred from the presence of desiccation cracks, blocky and prismatic structure, slickensides and carbonate nodules, all of which characterize present-day vertisols (FitzPatrick, 1980).

Fluvial channels of the Lower and Upper members contain large tree-trunk fragments. Their sizes imply the existence of vegetated channel margins, or high rates of precipitation in the source area. We favour the former interpretation, based on (a) the good preservation of the larger trunks at the margins of the channels, (b) the lacustrine facies interpretation, and (c) the common occurrence of densely vegetated banks of present-day rivers in semiarid and arid regions (e.g. Tooth and Nanson, 2000). The abundance of pedogenic carbonates in floodplain deposits of the Upper Member reflects an excess of alkaline solutions and oscillation of the water table, which could constitute evidence of increasing aridity during deposition of the unit. By contrast, there are no appreciable changes in the size of the sandbodies within the unit, which suggest no substantial changes in discharge. Fluctuations of the water table and variable (seasonal?) runoff could account for low organic-matter content and for the absence of coal in the floodplain deposits (McCabe and Parrish, 1992), owing to degradation of organic-matter during dry seasons. Meandering channels located in the Upper Member show in-channel mud deposition, which reflects occasional desiccation of the channel bed in response to a seasonal or ephemeral supply of water and sediment.

7.4. Volcanism

Evidence of intermittent volcanic activity during deposition of the Chubut Group comprises fine-grained pyroclastic beds and locally ignimbrites (Sciutto, 1981;

Fitzgerald et al., 1990; Figari et al., 1999; Bridge et al., 2000; Genise et al., 2002). Most of the volcanic deposits in the Matasiete Fm reflect distal (pyroclastic) events related to the early stages of uplift and deformation of the Andean Chain, located 150–200 km westward of the San Bernardo Fold Belt. Of particular interest are the pyroclastic surges identified in the upper part of the Middle Member in view of the inferred location of the Cretaceous volcanic centres. The geometry and lateral extent of surges depend on the type of surge, the topographical control and post-depositional erosion (Cas and Wright, 1987), but studies of recent eruptions indicate that maintenance of turbulent suspension of clasts over distances longer than 30 km is rare. A nearby source of the surge deposits exposed at the Matasiete Canyon is inferred from the tuff-dominated surge composition with well-preserved glass shards, the dominance of dune forms and wavy layering generated by turbulent flows, and the presence of accidental clasts and accretionary lapilli.

The abrupt increase in the *W*/*T* ratio of sandbodies deposited directly on top of pyroclastic beds in the Middle and Upper Member is interpreted as a direct consequence of the deposition of large quantities of pyroclastic material on the floodplain and inside channels, which produced several interrelated changes in the river system (Fig. 15). Firstly, sediment load abruptly increased due to the supply of large quantities of loosely consolidated material, either by fluvial processes or by heavy rains. Additionally, the low permeability of the fine-grained tephra relative to soils (Swanson et al., 1982; Smith, 1991) reduced the infiltration capacity of the floodplain and produced an increase in the runoff. The high aggradation rate of the floodplain and the increase of volume and variability of the sediment load could have increased the avulsion frequency and produced the observed widening of the sandbodies (Vessell and Davies, 1981).

In contrast to the widely acknowledged importance of tectonic and climate controls on the evolution of continental systems, our field data indicate that episodic input of pyroclastic material into the basin produced the most dramatic changes in fluvial architecture of the Matasiete Formation. However, these changes only temporarily affected the fluvial system, as demonstrated by the rapid return to previous geometries and sizes of the channelized sandbodies.

8. Conclusions

Detailed studies of lithofacies and facies associations in the Pozo D-129-Matasiete depositional system (Hauterivian–Aptian) have been carried out in the San Bernardo Fold Belt, where seventeen epiclastic, chemical and pyroclastic lithofacies were identified. Two facies associations were identified in the Pozo D-129 Fm, which represent shallow and deep-lacustrine environments. Five facies associations were identified in the fluvial Matasiete Fm: single fluvial channels, multistorey fluvial channels, proximal floodplain, distal floodplain, and pyroclastic deposits.

The lacustrine system of the Pozo D-129 Fm developed under semiarid climate conditions in a basin without connection to the sea. The lacustrine rocks in the San Bernardo Fold Belt indicate low gradient basin margins, coarsening-upward and shallowing facies trends and occasional excess of alkaline solutions, with precipitation of oolitic grainstones.

Near the basin margin, the fluvial Matasiete Fm is represented by single or multistorey channels encased in red and yellow–brown coloured floodplain fines with occasional pyroclastic deposits. The most complete section of the unit is exposed in the Matasiete Canyon, where it reaches a thickness of 650 m, and three members (Lower, Middle and Upper Member) have been distinguished based on stacking patterns and mudstone to sandstone ratio.

The Lower Member consists of a 205 m thick section, with three main channel belts separated by thick floodplain deposits. Most channels of this Member are coarse-grained (pebble conglomerates and coarse sandstones), with low dispersion (<50°) of paleocurrents. However, the channel belts show near-orthogonal changes in paleoflow directions. In-channel dunes are common in single and multistorey channels. They display rare fining-upward trends and occasional sedimentary structures generated under low-velocity conditions. Desiccation cracks are preserved on top of some multistorey channels, suggesting variable runoff and complete desiccation of the channel bed. Most channels are straight and appear to have migrated by avulsion during floods.

The Middle Member is a 215 m thick section dominated by floodplain deposition in laterally extensive, very shallow-waters or in vegetated lowlands. Several sandbodies are coarse-grained, lenticular, and have no diagnostic features. The paleotransport direction was to the south, and most of the bodies display low paleocurrent variability. The *W*/*T* ratio is variable through the Member, but the largest *W*/*T* ratio is recorded directly on top of tabular, pyroclastic surges, which appear to have provoked a modification of the channels from narrow ribbons to wider and shallower braided rivers.

The Upper Member consists of a 230 m thick section containing isolated sandbodies encased in thick red-coloured floodplain deposits. Channels with straight, meandering or braided behaviour are recorded in different

sections of the Member at the San Bernardo Fold Belt. Transportation was to the south with a considerable dispersion in individual sandbodies. The scarce multistorey channels with meandering behaviour reveal occasional desiccation of the channel bed. Paleosols analyzed in the floodplain of the Upper Member could be considered as vertisols, due to the presence of deep desiccation cracks and slickensides, as well as the abundance of carbonate concretions and caliche horizons. These features reflect oscillations of the water table, an excess of alkaline solutions and a semiarid (seasonal) climate. The absence of coal and the low organic-matter content suggest variable runoff and degradation of organic-matter during dry seasons. Tree trunks up to 1 m in diameter and 15 m long, preferentially located near channel margins, provide evidence for vegetated riverbanks.

The most dramatic changes in fluvial architecture were provoked by intermittent pyroclastic deposition on the floodplain. The fluvial system changed from single, ribbon channels to a short-lived braided river, which notably increased the *W*/*T* ratio of sandbodies. The reduced infiltration capacity of the floodplain and the concomitant increase in sediment load increased runoff, as well as volume and flashiness of the discharge, which favoured the development of shallow, multichannel rivers.

Acknowledgements

We are indebted to Jorge F. Rodriguez, René E. Hudecek and Raúl E. Giacosa for field assistance and constructive discussions. We thank V. Funes for XRD analysis, M. Barquín and A. Saiz (Chemical Department, UNPSJB) for chemical determinations and XRF analysis in paleosol samples. The Departamento de Geología of the UNPSJB is acknowledged for logistic support. This paper is a contribution to the PI CIUNPAT 521. Partial funding by the Research Project BTE2002-04316-C03-01 and Acción Complementaria CGL-2004-20409 del Ministerio de Educación y Ciencia, Spain, and by the Grup de Qualitat de la Generalitat de Catalunya, DURSI, 2001-SGR-00074 are gratefully acknowledged. The comments of two anonymous reviewers contributed to the clarity of this paper. Editors Gert Jan Weltje and Christopher Fielding are thanked for their very constructive comments and editorial assistance.

References

Abdul Aziz, H., Sanz-Rubio, E., Calvo, J.P., Hilgen, F.J., Krijgsman, W., 2003. Palaeoenvironmental reconstruction of a middle Miocene alluvial fan to cyclic shallow lacustrine depositional system in the Calatayud Basin (NE Spain). Sedimentology 50, 211–236.

Alexander, J., Leeder, M.R., 1987. Active tectonic control on alluvial architecture. In: Ethridge, F.G., Flores, R.M., Harvey, M.D. (Eds.), Recent Developments in Fluvial Sedimentology. Special Publication, vol. 39. Society of Economic Paleontologists and Mineralogists, pp. 243–259.

Alexander, J., Bridge, J.S., Cheel, R.J., LeClair, S.F., 2001. Bedforms and associated sedimentary structures formed under supercritical water flows over aggrading sand beds. Sedimentology 48, 133–152.

Allen, J.R.L., 1983. Studies in fluviatile sedimentation: bars, bar-complexes and sandstone sheets (low sinuosity braided streams) in the Brownstones (L. Devonian), Welsh Borders. Sedimentary Geology 33, 237–293.

Allen, J.R.L., 1986. Pedogenic calcretes in the Old Red Sandstone facies (Late Silurian–Early Carboniferous) of the Anglo-Welsh area, southern Britain. In: Wright, V.P. (Ed.), Paleosols: Their Recognition and Interpretation. Princeton Univ. Press, Princeton, NJ, pp. 139–179.

Archangelski, S., Baldón, A., Gamerro, J.C., Séller, J., 1984. Palinología estratigráfica del Cretácico de Argentina Austral. III. Distribución de las especies y conclusiones. Ameghiniana 21, 15–33.

Arche, A., Lopez-Gomez, J., 1999. Tectonic and geomorphic controls on the fluvial styles of the Eslida Formation, Middle Triassic, Eastern Spain. Tectonophysics 315, 187–207.

Barcat, C., Cortiñas, J., Nevistic, V., Zucchi, H., 1989. Cuenca del Golfo San Jorge. In: Chebli, G., Spalletti, L. (Eds.), Cuencas Sedimentarias Argentinas, pp. 319–345.

Bellosi, E.S., Gonzalez, M., Genise, J., 2002. Paleosuelos y sedimentación cretácica de la cuenca San Jorge (Grupo Chubut) en la Sierra de San Bernardo, Patagonia Central. 15° Congreso Geológico Argentino, vol. 2, 747–753 (Calafate).

Birkeland, P.W., 1984. Soils and Geomorphology. Oxford Univ. Press, Oxford. 372 pp.

Blum, M.D., Tornqvist, T.E., 2000. Fluvial response to sea-level change: a review and look forward. Sedimentology 47, 2–48.

Bridge, J.S., 1993. Description and interpretation of fluvial deposits: a critical perspective. Sedimentology 40, 801–810.

Bridge, J.S., Leeder, M.R., 1979. A simulation model of alluvial stratigraphy. Sedimentology 26, 617–644.

Bridge, J.S., Jalfin, G.A., Georgieff, S.M., 2000. Geometry, lithofacies, and spatial distribution of Cretaceous fluvial sandstone bodies, San Jorge Basin, Argentine: outcrops analog for the hydrocarbon-bearing Chubut Group. Journal of Sedimentary Research 70, 319–337.

Bristow, C.S., 1987. Brahmaputra River: channel migration and deposition. In: Ethridge, F.G., Flores, R.M., Harvey, M.D. (Eds.), Recent Developments in Fluvial Sedimentology. Special Publication, vol. 39. Society of Economic Paleontologists and Mineralogists, pp. 63–74.

Carey, S.N., 1991. Transport and deposition of thepra by pyroclastic flows and surges. In: Fisher, R.V., Smith, G.A. (Eds.), Sedimentation in Volcanic Settings. Special Publication, vol. 45. Society of Economic Paleontologists and Mineralogists, pp. 39–57.

Cas, R.A., Wright, J.V., 1987. Volcanic Successions, Modern and Ancient. Allen and Unwin, London. 528 pp.

Cecil, N., 2003. The concept of autocyclic and allocyclic controls on sedimentation and stratigraphy, emphasizing the climatic variable. In: Blaine Cecil, N., Terence Edgar, N. (Eds.), Climate Controls on Stratigraphy. Special Publication, vol. 77. Society of Economic Paleontologists and Mineralogists, pp. 13–20.

Clavijo, R., 1986. Estratigrafía del cretácico inferior en el sector occidental de la Cuenca Golfo San Jorge. Boletín de Informaciones Petroleras 9, 15–32 (Buenos Aires).

Collinson, J.D., 1996. Alluvial sediments, In: Reading, H.G. (Ed.), Sedimentary Environments: Processes, Facies and Stratigraphy, 3rd Ed. Blackwell, Oxford, pp. 37–82.

Cornell, R.M., Schwertmann, U., 2003. The Iron Oxides: Structure, Properties, Reactions, Occurrences, and Uses. Wiley-VCH, Weinheim. 664 pp.

Emery, D., Myers, K., 1996. Sequence Stratigraphy. Blackwell, Oxford. 297 pp.

Feruglio, E., 1949. Descripción Geológica de la Patagonia. Yacimientos Petrolíferos Fiscales 1, 1–334 (Buenos Aires).

Fielding, C.R., 2006. Upper flow regime sheets, lenses and scout-fills: extending the range of architectural elements for fluvial sediment bodies. Sedimentary Geology 190, 227–240.

Figari, E., Strelkov, E., Laffife, G., Cid de la Paz, M., Courtade, S., Celaya, J., Vottero, A., Lafourcade, P., Martinez, R., Villar, H., 1999. Los sistemas petroleros de la Cuenca del Golfo San Jorge: Síntesis estructural, estratigráfica y geoquímica. 4° Congreso de Exploración y Desarrollo de Hidrocarburos, pp. 197–237.

Fisher, R.V., Schmincke, H.U., 1984. Pyroclastic Rocks. Springer-Verlag, Berlín. 472 pp.

Fisher, R.V., Smith, G.A. (Eds.), 1991. Sedimentation in Volcanic Settings. Special Publication, vol. 45. Society of Economic Paleontologists and Mineralogists, pp. 1–257.

Fitzgerald, M.G., Mitchum, R.M., Uliana, M.A., Biddle, K.T., 1990. Evolution of the San Jorge Basin, Argentina. American Association of Petroleum Geologists Bulletin 74, 879–920.

FitzPatrick, E.A., 1980. Soils. Longman, New York. 353 pp.

Folguera, A., Iannizzotto, N., 2004. The Lagos La Plata and Fontana fold-and-thrust belt: long-lived orogenesis at the edge of western Patagonia. Journal of South American Earth Sciences 16, 541–566.

Friend, P.F., 1983. Toward the field classification of alluvial architecture or sequence. In: Collinson, J.D., Lewin, J. (Eds.), Modern and Ancient Fluvial Systems. Special Publication, vol. 6. International Association of Sedimentologists, pp. 345–354.

Friend, P.F., Slater, M.J., Williams, R.C., 1979. Vertical and lateral building of river sandstone bodies, Ebro basin, Spain. Journal of the Geological Society (London) 136, 39–46.

Galeazzi, J.S., 1989. Análisis de facies y paleocorrientes de la Formación Matasiete en la sección Sur del Cañadón homónimo: Sierra de San Bernardo, Chubut, Argentina. Msc. Thesis, UBA. Buenos Aires, Argentina, pp. 182.

Gawthorpe, R.L., Leeder, M., 2000. Tectono-sedimentary evolution of active extensional basins. Basin Research 12fs, 195–218.

Genise, J.F., Sciutto, J.C., Laza, J.H., Gonzalez, M.G., Bellosi, E.S., 2002. Fossil bee nests, coleopteral pupal chambers and tuffaceous paleosols from the Late Cretaceous Laguna Palacios Formation, Central Patagonia (Argentina). Palaeogeography, Palaeoclimatology, Palaeoecology 177, 215–235.

Hechem, J.J., 1994. Modelo predictivo de reservorios en un sistema fluvial efímero del Chubutiano de la cuenca del Golfo San Jorge, Argentina. Asociación Argentina de Sedimentología Revista 1, 3–14.

Hechem, J.J., 1998. Arquitectura y paleodrenaje del sistema fluvial efímero de la Formación Bajo Barreal, cuenca del Golfo San Jorge, Argentina. 1° Congreso Latinoamericano de Sedimentología, pp. 315–323. Isla Margarita.

Hechem, J.J., Strelkov, E.E., 2002. Secuencia sedimentaria mesozoica del Golfo San Jorge. In: Haller, J.M. (Ed.), Geología y recursos Naturales de Santa Cruz. 15° Congreso Geológico Argentino, vol. 1, pp. 129–147. Buenos Aires.

Hechem, J.J., Figari, E.G., Musacchio, E.A., 1987. Hallazgo de la Formación Pozo D-129. Petrotecnia 28 (11), 13–15.

Hechem, J.J., Homovc, J.F., Figari, E.G., 1990. Estratigrafía del Chubutiano (Cretácico) en la Sierra de San Bernardo, cuenca del Golfo San Jorge, Argentina. 11° Congreso Geológico Argentino, vol. 3, pp. 173–176. San Juan.

Holbrook, J., Schumm, S.A., 1999. Geomorphic and sedimentary response of rivers to tectonic deformation: a brief review and critique of a tool for recognizing subtle epeirogenic deformation in modern and ancient settings. Tectonophysics 305, 287–306.

Homovc, J.F., Conforto, G.A., Lafourcade, P.A., Chelotti, L.A., 1995. Fold belt in the San Jorge Basin, Argentine: an example of tectonic inversion. In: Buchanan, J.G., Buchanan, P.G. (Eds.), Basin Inversion. Special Publication, vol. 88. Geological Society of London, pp. 235–248.

Klappa, C.F., 1980. Rhizoliths in terrestrial carbonates: classification, recognition, genesis and significance. Sedimentology 26, 613–629.

Kraus, M.J., 1999. Paleosols in clastic sedimentary rocks: their geological applications. Earth-Science Reviews 47, 41–70.

Kraus, M.J., Hasiotis, S.T., 2006. Significance of different modes of rhizolith preservation to interpreting paleoenvironmental and paleohydrologic settings: examples from Paleogene paleosols, Bighorn basin, Wyoming U.S.A. Journal of Sedimentary Research 76, 633–646.

Leeder, M.R., Steward, M.D., 1996. Fluvial incision and sequence stratigraphy: alluvial responses to relative sea-level fall and their detection in the geological record. In: Hesselbo, S.P., Parkinson, D.N. (Eds.), Sequence Stratigraphy in British Geology. Special Publication, vol. 103. Geological Society of London, pp. 25–39.

Legarreta, L., Uliana, M., 1998. Anatomy of hinterland depositional sequences: Upper Cretaceous fluvial strata, Neuquén basin, West-central, Argentina. In: Shanley, K., McCabe, P. (Eds.), Relative Role of Eustasy, Climate and Tectonism in Continental Rocks. Special Publication, vol. 59. Society of Economic Paleontologists and Mineralogists, pp. 83–92.

Legarreta, L., Uliana, M., Larotonda, C.A., Meconi, G.R., 1993. Approaches to nonmarine sequence stratigraphy — theoretical models and examples from Argentine basins. In: Eschard, R., Doliez, B. (Eds.), Subsurface Reservoir Characterization from Outcrop Observations. Collection Colloques et Séminaires, vol. 51. Editions Technip, Paris, pp. 125–145.

Lesta, P., Ferello, R., 1972. Región Extraandina del Chubut y norte de Santa Cruz. In: Leanza, A., Academia Nacional de Ciencias (Eds.) Geología Regional Argentina: 601–654. Córdoba.

Link, M.H., Osborne, R.H., 1978. Lacustrine facies in the Pliocene Ridge basin, California. In: Matter, A., Tucker, M.E. (Eds.), Modern and Ancient Lake Sediments. Special Publication, vol. 2. International Association of Sedimentologists, pp. 167–187.

Lunt, I.A, Bridge, J.S., Tye, R.S., 2004. A quantitative, three dimensional depositional model of gravely braided rivers. Sedimentology 51, 377–414.

Machette, M.N., 1985. Calcic soils of the southwestern United States. In: Weide, D.L. (Ed.), Soils and Quaternary Geology of the South West United States. Special Paper, vol. 203. Geological Society of America, pp. 1–21.

Makaske, B., 2001. Anastomosing rivers: a review of their classification, origin and sedimentary products. Earth-Science Reviews 53, 149–196.

Marriot, S.B., Wright, V.P., 1993. Paleosols as indicators of geomorphic stability in two Old Red Sandstone alluvial suites, South Wales. Journal of the Geological Society (London) 150, 1109–1120.

Mathisen, M.E., Vondra, C.F., 1983. The fluvial and pyroclastic deposits of the Cagayan Basin, northern Luzon, Philippines — an example of nonmarine volcaniclastic sedimentation in an interarc basin. Sedimentology 30, 369–392.

McCabe, P.J., Parrish, J.T., 1992. Tectonic and climatic controls on the distribution of Cretaceous coals. In: McCabe, P.J., Parrish, J.T. (Eds.), Controls on the Distribution and Quality of Cretaceous Coals. Special Paper, vol. 267. Geological Society of America, pp. 1–15.

Meconi, G., 1990. Facies, arquitectura fluvial y paleoambientes del Grupo Chubut en el Codo del Río Senguer, límite provincial de Chubut-Santa Cruz. 3° Reunión Argentina de Sedimentología, pp. 193–196. San Juan.

Miall, A.D., 1996. The Geology of Fluvial Deposits: Sedimentary Facies, Basin Analysis and Petroleum Geology. Springer-Verlag, Berlin. 582 pp.

Nadon, G.C., 1994. The genesis and recognition of anastomosed fluvial deposits: data from the St. Mary River formation, Southwestern Alberta, Canada. Journal of Sedimentary Petrology 64, 451–463.

Nanson, G.C., Croke, J.C., 1992. A genetic classification of floodplains. Geomorphology 4, 459–486.

Nanson, G.C., Knighton, A.D., 1996. Anabranching rivers: their cause, character and classification. Earth Surface Processes and Landforms 21, 217–239.

Paredes, J.M., Hudecek, R., Foix, N., Rodriguez, J.F., Nillni, A., 2003. Análisis paleoambiental de la Formación Matasiete (Aptiano) en su área tipo, noroeste de la Cuenca del Golfo San Jorge, Argentina. Asociación Argentina de Sedimentología Revista 10, 82–101.

Paredes, J.M., Foix, N., Hudecek, R., Rodriguez, J.F.R., Nillni, A., 2004. Arquitectura y estilos fluviales de la Formación Matasiete, Aptiano de la Cuenca del Golfo San Jorge, Argentina. 10° Reunión Argentina de Sedimentología, pp. 129–130. San Luis.

Peroni, G., Hegedus, A., Cerdan, J., Legarreta, L., Uliana, M., Laffite, G., 1995. Hydrocarbon accumulation in an inverted segment of the Andean Foreland: San Bernardo Belt, Central Patagonia. In: Tankard, A., Suarez, R., Welsink, H. (Eds.), Petroleum basins of South America. American Association of Petroleum Geologists Bulletin, vol. 62, pp. 403–419.

Platt, N.H., Wright, V.P., 1991. Lacustrine carbonates: facies models, facies distributions and hydrocarbon aspects. In: Anadón, P., Cabrera, L., Kelts, K. (Eds.), Lacustrine Facies Analysis. Special Publication, vol. 13. International Association of Sedimentologists, pp. 57–74.

Ramsay, J.G., 1961. The effects of folding upon the orientation of sedimentary structures. Journal of Geology 69, 84–100.

Retallack, G.J., 1988. Field recognition of paleosols. In: Reinhardt, J., Sigleo, W.R. (Eds.), Paleosols and Weathering Through Geologic Time: Principles and Applications. Special Paper, vol. 216. Geological Society of America, pp. 1–20.

Retallack, G.J., 1990. Soils of the Past. Unwin-Hyman, London. 520 pp.

Rodriguez, J.F., 1992. Interpretación paleoambiental de la Formación Bajo Barreal (Cretácico tardío) en Estancia Ocho Hermanos, Chubut. 4° Reunión Argentina de Sedimentología, vol. 2, pp. 81–88. La Plata.

Rodriguez, J.F., Littke, R., 2001. Petroleum generation and accumulation in the Golfo San Jorge Basin, Argentina: a basin modeling study. Marine and Petroleum Geology 18, 995–1028.

Rust, B.R., 1978. A classification of alluvial channels systems. In: Miall, A.D. (Ed.), Fluvial Sedimentology. Canadian Society of Petroleum Geology, Memoir, vol. 5, pp. 187–198.

Schumacher, R., Schmincke, H.U., 1995. Models for the origin of accretionary lapilli. Bulletin of Volcanology 56, 626–639.

Schumm, S.A., 1963. A tentative classification of alluvial river channels. US Geological Survey Circular 477.

Schumm, S.A., 1977. The Fluvial System. Wiley, New York. 338 pp.

Schumm, S.A., 1993. River response to baselevel change: implication for basin stratigraphy. Journal of Geology 101, 279–294.

Sciutto, J.C., 1981. Geología del Codo del Río Senguerr, Chubut, Argentina. 8° Congreso Geológico Argentino, vol. 3, pp. 203–219. San Luis.

Sciutto, J.C., Martínez, R.D., 1996. El Grupo Chubut en el Anticlinal Sierra Nevada, Chubut, Argentina. 8° Congreso Geológico Argentino y 3° Congreso Geológico de Exploración de Hidrocarburos, vol. 1, pp. 67–75. Salta.

Shanley, K.W., McCabe, P.J., 1994. Perspectives on the sequence stratigraphy of continental strata. American Association of Petroleum Geologists Bulletin 78, 544–568.

Shanley, K.W., McCabe, P., 1998. Relative role of eustasy. Climate and Tectonism in Continental Rocks. Special Publication, vol. 59. Society of Economic Paleontologists and Mineralogists, pp. 1–234.

Slingerland, R., Smith, N.D., 2004. River avulsion and their deposits. Annual Review of Earth and Planetary Sciences 32, 257–285.

Smith, G.A., 1987. The influence of explosive volcanism on fluvial sedimentation: the Deschutes Formation (Neogene) in central Oregon. Journal of Sedimentary Petrology 57, 613–629.

Smith, G.A., 1991. Facies sequences and geometries in continental volcaniclastic sediments. In: Fisher, R.V., Smith, G.A. (Eds.), Sedimentation in Volcanic Settings. Special Publication, vol. 45. Society of Economic Paleontologists and Mineralogists, pp. 109–121.

Smith, N.D., Cross, T.A., Dufficy, J.P., Clough, S.R., 1989. Anatomy of an avulsion. Sedimentology 36, 1–24.

Swanson, F.J., Collins, B., Dunne, T., Wicherski, B.P., 1982. Erosion of tephra from hillslopes near Mt. St. Helens and other volcanoes. Proceedings of the Symposium on Erosion Control in Volcanic Areas, Public Works Research Institute, Japan, Technical Memorandum, vol. 1908, pp. 183–221.

Talbot, M.R., Allen, P.A., 1996. Lakes, In: Reading, H.G. (Ed.), Sedimentary Environments: Processes, Facies and Stratigraphy, 3rd Ed. Blackwell, Oxford, pp. 83–124.

Tooth, S., Nanson, G.C., 1999. Anabranching rivers on the Northern Plains of arid central Australia. Geomorphology 29, 211–233.

Tooth, S., Nanson, G.C., 2000. The role of vegetation in the formation of anabranching channels in an ephemeral river, Northern plains, arid central Australia. Hydrological Processes 14, 3099–3117.

Uliana, M., Legarreta, L., 1999. Jurásico y Cretácico de la Cuenca del Golfo San Jorge. In: Caminos, R. (Ed.), Geología Argentina. Subsecretaría de Minería de la Nación, Buenos Aires, pp. 496–510.

Van Nieuwenhuise, D.S., Ormiston, A.R., 1989. A model for the origin of source-rich lacustrine facies, San Jorge Basin, Argentina. 1° Congreso Nacional de Exploración de Hidrocarburos, vol. 2, pp. 853–883.

Vessell, R.K., Davies, D.K., 1981. Non-marine sedimentation in an active forearc basin. In: Ethridge, F.G., Flores, R.M. (Eds.), Recent and Ancient Nonmarine Depositional Environments: Model for Exploration. Special Publication, vol. 31. Society of Economic Paleontologists and Mineralogists, pp. 31–45.

Woolfe, N.J., Balzary, J.R., 1996. Fields in the spectrum of channel style. Sedimentology 43, 797–805.

Wright, D., 1999. The role of sulphate-reducing bacteria and cyanobacteria in dolomite formation in distal ephemeral lakes of the Coorong region, South Australia. Sedimentary Geology 126, 147–157.

Wright, V.P., Marriot, S.B., 1993. The sequence stratigraphy of fluvial depositional systems: the role of floodplain sediment storage. Sedimentary Geology 86, 203–210.